conditions and identified simple input–output relationships based on ligand/receptor and transcription/anti-pathogen activities, respectively, by optimizing the signaling flux with respect to the output flux. This procedure significantly reduced the complexity of the full network consisting of 752 distinct chemical species and 909 reactions into 41 relationships between 14 receptors and 6 outputs. They further simplified the network by identifying redundant pathways and identified eight critical biochemical reactions, which specifically affect the pathways of reactive oxygen species (ROS), IL-1-induced NF-kB activation and MyD88-mediated NF-kB/AP-1 activation. Because it is not yet clear how analyses based on steady-state behavior like FBA apply to the dynamics of TLR signal transduction networks, it will be important to validate such predictions experimentally. In addition, some of the discussion in Ref 35 was apparently based on an earlier misidentification of TLR2 as an LPS receptor, which has been subsequently shown to be a result of contamination. Thus, in spite of the great effort made in curating the original network, this example indicates that continuous collaboration between experts in computational and immunology fields is very important.

Combining Gene Expression and Regulatory Sequence Motifs

While the above network models are based on known components and topologies of TLR signal transduction, it is of great interest to infer the yet unknown components and regulatory relationships by computational approaches. A strategy often used is to predict shared regulatory motifs in the regulatory regions of co-expressed genes (Box 2). Despite the apparent simplicity of this approach, it is hampered in practice by the low specificity and sensitivity of transcription factor binding site (TFBS) prediction using position weight matrices (PWMs)[36] (see Box 1). Nevertheless, because experimental identification of regulatory sites is expensive and labor intensive, computational predictions are often used to provide a first hint or hypothesis, which can subsequently be tested by wet lab experiments. An example of one such study started from sets of genes with similar expression profiles in macrophages after TLR stimulation.[37] The authors next scanned promoter sequences of these genes with a set of PWMs, and identified possible regulatory relationships between TFs and clusters of co-regulated genes. These relationships were subsequently combined with additional gene expression data in order to predict causal relationships between regulators and target genes. An important detail was their use of time-lagged correlation between the expression of TFs and their candidate target genes, allowing for the prediction of causal TF-target relationships. Among the important genes they identified, known regulators, such as NF-kB, interferon regulatory factors (IRFs), and AP-1, were found as well as a previously unidentified regulator, TGIF1.

Rather than attempting to explain the regulation of transcription on a large scale, some studies have performed detailed dissection of a small set of genes or regulatory sites. In one such study, Leung and coworkers focused on genes that are under the regulation of two NF-kB binding sites.[44] They found that in these genes both sites are required for the

BOX 2

BASIC REGULATORY NETWORK INFERENCE STRATEGIES

Network inference approaches utilize large-scale sequence and expression data to reconstruct biological networks. A relatively simple approach to network inference is based on the assumption that co-expressed pairs of genes have some level of interaction (Figure 4). Typically, a pairwise comparison of the expression profiles of all genes is made, and a network is constructed where each pair of significantly correlated genes is connected by an edge. Importantly, correlation of expression does not necessarily imply a causal relationship, and is not able to distinguish direct interactions from indirect ones. A number of strategies have been developed that attempt to solve the above problem, such as the use of time-lagged correlation of expression, and various integrative approaches.[38] The latter typically use transcription factor binding sites in the regulatory regions of target genes to predict direct regulatory interactions (Figure 4). Although a number of successful applications to mammalian data have been reported,[37,39] noisy expression data and the relatively small size of regulatory sites make network inference a non-trivial problem. In addition, the use of mRNA levels as estimator for gene activity introduces an additional layer of complexity, as regulation of translation, post-translational modifications, and cellular localization are known to play an important role in the regulation of gene activity.[40,41] Here, further advances in measuring protein abundance and post-translational modifications,[42] such as phosphorylation[43] will allow for a better understanding of TLR signaling.

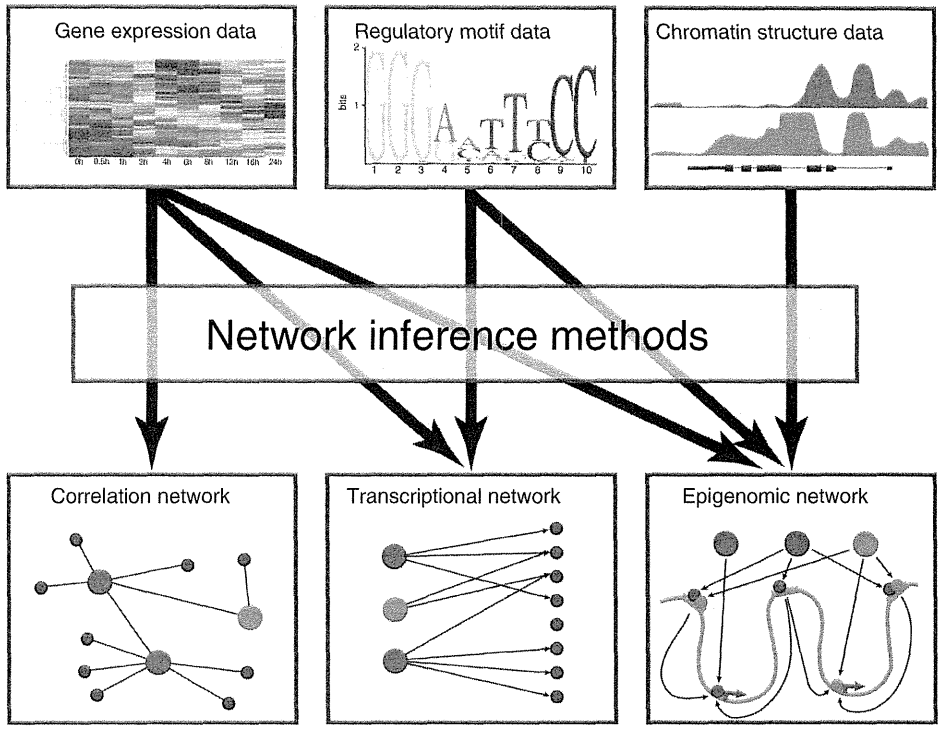

FIGURE 4 | Levels of complexity in network inference. By integration of additional types of data with expression data, the inference of increasingly complex networks becomes possible. Regulatory motif data can be used to add directionality to gene expression-based networks, while increasing amounts of epigenetic data will in the near future allow us to construct genome-wide networks including distal regulatory enhancers as well as traditional network components.

activity of the gene, and that swapping the sites alters the NF-kB family members that bind to them. More importantly, they found that the combination of the two sites affects which coactivator binds to the bound NF-kB dimer, and that even a single nucleotide within the NF-kB site can change the cofactor specificity. In another study, Giorgetti and colleagues showed that clusters of NF-kB binding sites could be used in a non-cooperative way to process increasing levels of NF-kB into gradual increments of transcriptional response.[45] This result was in sharp contrast with the widely accepted view that graded increases in TF concentration result—through cooperative binding—in a digital transcription initiation signal. These two findings are indicative of a wide variety of features that contribute to different transcriptional responses.

Network Inference from Large-Scale Perturbations

A number of studies have analyzed the activity of transcriptional regulators by systematic perturbation experiments. Recently, for example, Amit and coworkers reconstructed the regulatory relationships among transcripts whose expression levels depend on TLR stimulation.[46] They observed transcriptional expression levels for 118 predetermined target genes 6 h after LPS stimulation in dendritic cells. The cells were independently perturbed using small hairpin RNA (shRNA) for 144 candidate regulators. The resulting gene expression levels were used to define statistically significant activating and repressing relationships between regulators and target genes. As a result, they identified 1728 activations and 594 repressions. Although their results likely contain a significant number of indirect regulations, their study nevertheless quantified interactions between components in the inflammatory and antiviral programs of dendritic cells with unprecedented breadth. This is an example where, in the case of DNA-binding proteins, sequence analysis or ChIP-seq experiments, discussed below, might help to distinguish between direct and indirect interactions. Using a similar perturbation approach, along with predicted TF activities, Suzuki and coworkers examined 52 TFs in human myeloid leukaemia cells.[47] In these perturbation studies, genome-wide data were first used to select a smaller set of representative genes. These representatives included candidate regulators for perturbation experiments, and also a

subset of genes for which expression changes will be measured. Narrowing down the number of genes of interest is an important step because it maximizes the information obtained from a given experiment. Although cell types and stimuli were different, the results of both studies suggest that the gene expression in a single immune cell type is controlled by a substantial number of core regulators and additional fine-tuners.

Future Perspectives

Although most studies on the regulation of transcription have focused on the roles of TFs and their binding sites, additional levels of regulation exist, one being the structural state of the chromatin (Figure 4). Transcription can be regulated on an epigenetic level by various mechanisms (see reviews 11, 48), and it is likely that some TFs are associated with different epigenetic changes. Importantly, it has become clear that primary (or immediate-early) response genes and secondary response genes in TLR signaling differ fundamentally in their chromatin structure, as well as their tendencies to have preassembled RNA-polymerase II at their promoters, dependence on chromatin remodeling for induction, and association with CpG islands.[49–51] Although a number of studies have elucidated interactions between TFs and histone modifiers,[52–56] in general, the causal relationships between these features are still unclear. Nevertheless, our current understanding suggests that any approach aiming at modeling or explaining the dynamics of gene expression during the immune response should try to incorporate the fact that several classes and subclasses of regulatory regions exist, and that they are likely to be under the control of fundamentally different regulatory mechanisms (see review 48).

Recent studies have attempted to combine chromatin structure and histone modification data with the analysis of regulatory networks. In general, these approaches aim to use epigenetic features as a measure of accessibility of DNA sequences or activity of genes, and to use this as prior knowledge in the discovery of regulatory motifs. One example is the study by Ramsey et al.[57] who focused specifically on macrophages. After combining ChIP-seq data for a number of TFs with histone acetylation (HAc) data, the authors observed that TFBSs often occur within local minima of HAc ChIP-seq signals within HAc-rich regions. Based on this observation they defined a 'valley score' and they showed that the use of this score in combination with PWM scores could improve TFBS prediction accuracy. The improvement was variable from TF to TF though, suggesting that depending on the biological function of the TF, different epigenetic features might lead to better predictions. Approaches such as CENTIPEDE[58] and simpler methods[59] that aim to computationally predict TF binding events using a limited amount of experimental data yet with an accuracy similar to that of 'gold-standard' ChIP-seq experiments are therefore likely to continue to play an important role in system-level analyses of transcriptional regulation.

CONCLUSION

Computational modeling has played an important role in the study of TLR signaling. Since many of its components are shared between organisms as diverse as mice, insects, and worms, sequence homology has guided many pioneering experiments that have revealed key biochemical functions in these pathways. Computational analysis of the macromolecular structures along with site-directed mutagenesis has provided insight into the mechanism of signaling pathways in normal and diseased states. Accurate mathematical modeling of signal transduction dynamics is a challenging goal due to our incomplete knowledge of the components and their interactions. However, the general topology of the TLR signaling network in mammals has been established. Gene expression data in parallel with controlled perturbations will enable current models to be continuously refined. Extensions of these models wherein structural information is integrated with network-based signaling models are expected to provide a more quantitative description of TLR signaling in the future. The increasing number of public databases, such as the innateDB,[60] ImmGen[61] and Macrophages.com,[62] and tools[63,64] will enable further refinement by facilitating data sharing and interpretation, and establishing standards. Finally, it must be acknowledged that immunology is still very much an experimental discipline. The emergence of new experimental techniques, especially those that quantify gene and protein expression levels, as well as epigenetic and post-translational modifications, is expected to add depth to our understanding. However, we are convinced that in order to understand the immune response on a system's level, and the interactions between its various parts, the future contribution of computational methodologies will be invaluable. We believe that the studies we have discussed above will be a foundation for future developments.

REFERENCES

1. Moresco EM, LaVine D, Beutler B. Toll-like receptors. *Curr Biol* 2011, 21:R488–R493.
2. Takeuchi O, Akira S. Pattern recognition receptors and inflammation. *Cell* 2010, 140:805–820.
3. Adachi O, Kawai T, Takeda K, Matsumoto M, Tsutsui H, Sakagami M, Nakanishi K, Akira S. Targeted disruption of the MyD88 gene results in loss of IL-1- and IL-18-mediated function. *Immunity* 1998, 9:143–150.
4. Yamamoto M, Sato S, Hemmi H, Hoshino K, Kaisho T, Sanjo H, Takeuchi O, Sugiyama M, Okabe M, Takeda K, et al. Role of adaptor TRIF in the MyD88-independent toll-like receptor signaling pathway. *Science* 2003, 301:640–643.
5. Li S, Wang L, Berman M, Kong YY, Dorf ME. Mapping a dynamic innate immunity protein interaction network regulating type I interferon production. *Immunity* 2011, 35:426–440.
6. Bovijn C, Ulrichts P, De Smet AS, Catteeuw D, Beyaert R, Tavernier J, Peelman F. Identification of interaction sites for dimerization and adapter recruitment in the toll/interleukin-1 receptor (TIR) domain of toll-like receptor 4. *J Biol Chem* 2011, 287:4088–4098.
7. Nunez Miguel R, Wong J, Westoll JF, Brooks HJ, O'Neill LA, Gay NJ, Bryant CE, Monie TP. A dimer of the toll-like receptor 4 cytoplasmic domain provides a specific scaffold for the recruitment of signalling adaptor proteins. *PLoS One* 2007, 2:e788.
8. Valkov E, Stamp A, Dimaio F, Baker D, Verstak B, Roversi P, Kellie S, Sweet MJ, Mansell A, Gay NJ, et al. Crystal structure of toll-like receptor adaptor MAL/TIRAP reveals the molecular basis for signal transduction and disease protection. *Proc Natl Acad Sci U S A* 2011, 108:14879–14884.
9. Gay NJ, Gangloff M, O'Neill LA. What the myddosome structure tells us about the initiation of innate immunity. *Trends Immunol* 2011, 32:104–109.
10. Mariani V, Kiefer F, Schmidt T, Haas J, Schwede T. Assessment of template based protein structure predictions in CASP9. *Proteins* 2011, 79(suppl 10):37–58.
11. Lensink MF, Wodak SJ. Blind predictions of protein interfaces by docking calculations in CAPRI. *Proteins* 2010, 78:3085–3095.
12. Gillespie DT. Stochastic simulation of chemical kinetics. *Annu Rev Phys Chem* 2007, 58:35–55.
13. Orth JD, Thiele I, Palsson BO. What is flux balance analysis? *Nat Biotechnol* 2010, 28:245–248.
14. Stormo GD. DNA binding sites: representation and discovery. *Bioinformatics* 2000, 16:16–23.
15. Kim HM, Park BS, Kim JI, Kim SE, Lee J, Oh SC, Enkhbayar P, Matsushima N, Lee H, Yoo OJ, et al. Crystal structure of the TLR4-MD-2 complex with bound endotoxin antagonist Eritoran. *Cell* 2007, 130:906–917.
16. Nyman T, Stenmark P, Flodin S, Johansson I, Hammarstrom M, Nordlund P. The crystal structure of the human toll-like receptor 10 cytoplasmic domain reveals a putative signaling dimer. *J Biol Chem* 2008, 283:11861–11865.
17. Zhang Y, Gao X, Michael Garavito R. Structural analysis of the intracellular domain of (pro)renin receptor fused to maltose-binding protein. *Biochem Biophys Res Commun* 2011, 407:674–679.
18. Ohnishi H, Tochio H, Kato Z, Orii KE, Li A, Kimura T, Hiroaki H, Kondo N, Shirakawa M. Structural basis for the multiple interactions of the MyD88 TIR domain in TLR4 signaling. *Proc Natl Acad Sci U S A* 2009, 106:10260–10265.
19. Jin MS, Kim SE, Heo JY, Lee ME, Kim HM, Paik SG, Lee H, Lee JO. Crystal structure of the TLR1-TLR2 heterodimer induced by binding of a tri-acylated lipopeptide. *Cell* 2007, 130:1071–1082.
20. Kang JY, Nan X, Jin MS, Youn SJ, Ryu YH, Mah S, Han SH, Lee H, Paik SG, Lee JO. Recognition of lipopeptide patterns by toll-like receptor 2-toll-like receptor 6 heterodimer. *Immunity* 2009, 31:873–884.
21. Liu L, Botos I, Wang Y, Leonard JN, Shiloach J, Segal DM, Davies DR. Structural basis of toll-like receptor 3 signaling with double-stranded RNA. *Science* 2008, 320:379–381.
22. Yoon S-i, A Kurnasov O, A Natarajan V, A Hong M, A Gudkov AV, Osterman AL, Wilson IA. Structural basis of TLR5-flagellin recognition and signaling. *Science* 2012, 335:859–864.
23. Kubarenko AV, Ranjan S, Colak E, George J, Frank M, Weber AN. Comprehensive modeling and functional analysis of toll-like receptor ligand-recognition domains. *Protein Sci* 2010, 19:558–569.
24. Guan Y, Ranoa DR, Jiang S, Mutha SK, Li X, Baudry J, Tapping RI. Human TLRs 10 and 1 share common mechanisms of innate immune sensing but not signaling. *J Immunol* 2010, 184:5094–5103.
25. Hutchinson MR, Loram LC, Zhang Y, Shridhar M, Rezvani N, Berkelhammer D, Phipps S, Foster PS, Landgraf K, Falke JJ, et al. Evidence that tricyclic small molecules may possess toll-like receptor and myeloid differentiation protein 2 activity. *Neuroscience* 2010, 168:551–563.
26. Li Y, Efferson CL, Ramesh R, Peoples GE, Hwu P, Ioannides CG. A peptidoglycan monomer with the glutamine to serine change and basic peptides bind in silico to TLR-2 (403-455). *Cancer Immunol Immunother* 2010, 60:515–524.
27. Lin SC, Lo YC, Wu H. Helical assembly in the MyD88-IRAK4-IRAK2 complex in TLR/IL-1R signalling. *Nature* 2010, 465:885–890.
28. Hoffmann A, Levchenko A, Scott ML, Baltimore D. The IκB-NF-κB signaling module: temporal control

and selective gene activation. *Science* 2002, 298: 1241–1245.

29. Covert MW, Leung TH, Gaston JE, Baltimore D. Achieving stability of lipopolysaccharide-induced NF-kappaB activation. *Science* 2005, 309:1854–1857.
30. Werner SL, Barken D, Hoffmann A. Stimulus specificity of gene expression programs determined by temporal control of IKK activity. *Science* 2005, 309:1857–1861.
31. Shih VF, Kearns JD, Basak S, Savinova OV, Ghosh G, Hoffmann A. Kinetic control of negative feedback regulators of NF-kappaB/RelA determines their pathogen- and cytokine-receptor signaling specificity. *Proc Natl Acad Sci U S A* 2009, 106:9619–9624.
32. Cheong R, Hoffmann A, Levchenko A. Understanding NF-kappaB signaling via mathematical modeling. *Mol Syst Biol* 2008, 4:192.
33. Teraguchi S, Kumagai Y, Vandenbon A, Akira S, Standley DM. Stochastic binary modeling of cells in continuous time as an alternative to biochemical reaction equations. *Phys Rev E* 2011, 84:062903.
34. Oda K, Kitano H. A comprehensive map of the toll-like receptor signaling network. *Mol Syst Biol* 2006, 2:2006.0015.
35. Li F, Thiele I, Jamshidi N, Palsson BO. Identification of potential pathway mediation targets in Toll-like receptor signaling. *PLoS Comput Biol* 2009, 5:e1000292.
36. Wasserman WW, Sandelin A. Applied bioinformatics for the identification of regulatory elements. *Nat Rev Genet* 2004, 5:276–287.
37. Ramsey SA, Klemm SL, Zak DE, Kennedy KA, Thorsson V, Li B, Gilchrist M, Gold ES, Johnson CD, Litvak V, et al. Uncovering a macrophage transcriptional program by integrating evidence from motif scanning and expression dynamics. *PLoS Comput Biol* 2008, 4: e1000021.
38. De Smet R, Marchal K. Advantages and limitations of current network inference methods. *Nat Rev Microbiol* 2010, 8:717–729.
39. Basso K, Margolin AA, Stolovitzky G, Klein U, Dalla-Favera R, Califano A. Reverse engineering of regulatory networks in human B cells. *Nat Genet* 2005, 37: 382–390.
40. Honda K, Taniguchi T. IRFs: master regulators of signalling by Toll-like receptors and cytosolic pattern-recognition receptors. *Nat Rev Immunol* 2006, 6: 644–658.
41. Chen LF, Greene WC. Shaping the nuclear action of NF-kappaB. *Nat Rev Mol Cell Biol* 2004, 5:392–401.
42. Cox J, Mann M. Is proteomics the new genomics? *Cell* 2007, 130:395–398.
43. Weintz G, Olsen JV, Fruhauf K, Niedzielska M, Amit I, Jantsch J, Mages J, Frech C, Dolken L, Mann M, et al. The phosphoproteome of toll-like receptor-activated macrophages. *Mol Syst Biol* 2010, 6:371.
44. Leung TH, Hoffmann A, Baltimore D. One nucleotide in a kappa B site can determine cofactor specificity for NF-kappa B dimers. *Cell* 2004, 118:453–464.
45. Giorgetti L, Siggers T, Tiana G, Caprara G, Notarbartolo S, Corona T, Pasparakis M, Milani P, Bulyk ML, Natoli G. Noncooperative interactions between transcription factors and clustered DNA binding sites enable graded transcriptional responses to environmental inputs. *Mol Cell* 2010, 37:418–428.
46. Amit I, Garber M, Chevrier N, Leite AP, Donner Y, Eisenhaure T, Guttman M, Grenier JK, Li W, Zuk O, et al. Unbiased reconstruction of a mammalian transcriptional network mediating pathogen responses. *Science* 2009, 326:257–263.
47. Suzuki H, Forrest ARR, van Nimwegen E, Daub CO, Balwierz PJ, Irvine KM, Lassmann T, Ravasi T, Hasegawa Y, de Hoon MJL, et al. The transcriptional network that controls growth arrest and differentiation in a human myeloid leukemia cell line. *Nat Genet* 2009, 41:553–562.
48. Smale ST. Selective transcription in response to an inflammatory stimulus. *Cell* 2010, 140:833–844.
49. Hargreaves DC, Horng T, Medzhitov R. Control of inducible gene expression by signal-dependent transcriptional elongation. *Cell* 2009, 138:129–145.
50. Ramirez-Carrozzi VR, Braas D, Bhatt DM, Cheng CS, Hong C, Doty KR, Black JC, Hoffmann A, Carey M, Smale ST. A unifying model for the selective regulation of inducible transcription by CpG islands and nucleosome remodeling. *Cell* 2009, 138:114–128.
51. Ramirez-Carrozzi VR, Nazarian AA, Li CC, Gore SL, Sridharan R, Imbalzano AN, Smale ST. Selective and antagonistic functions of SWI/SNF and Mi-2 beta nucleosome remodeling complexes during an inflammatory response. *Gene Dev* 2006, 20:282–296.
52. Ishii M, Wen HT, Corsa CAS, Liu TJ, Coelho AL, Allen RM, Carson WF, Cavassani KA, Li XZ, Lukacs NW, et al. Epigenetic regulation of the alternatively activated macrophage phenotype. *Blood* 2009, 114:3244–3254.
53. Satoh T, Takeuchi O, Vandenbon A, Yasuda K, Tanaka Y, Kumagai Y, Miyake T, Matsushita K, Okazaki T, Saitoh T, et al. The Jmjd3-Irf4 axis regulates M2 macrophage polarization and host responses against helminth infection. *Nat Immunol* 2010, 11:936–U989.
54. De Santa F, Narang V, Yap ZH, Tusi BK, Burgold T, Austenaa L, Bucci G, Caganova M, Notarbartolo S, Casola S, et al. Jmjd3 contributes to the control of gene expression in LPS-activated macrophages. *EMBO J* 2009, 28:3341–3352.
55. De Santa F, Totaro MG, Prosperini E, Notarbartolo S, Testa G, Natoli G. The histone H3 lysine-27 demethylase Jmjd3 links inflammation to inhibition of polycomb-mediated gene silencing. *Cell* 2007, 130: 1083–1094.

56. Gilchrist M, Thorsson V, Li B, Rust AG, Korb M, Kennedy K, Hai T, Bolouri H, Aderem A. Systems biology approaches identify ATF3 as a negative regulator of Toll-like receptor 4. *Nature* 2006, 441:173–178.

57. Ramsey SA, Knijnenburg TA, Kennedy KA, Zak DE, Gilchrist M, Gold ES, Johnson CD, Lampano AE, Litvak V, Navarro G, et al. Genome-wide histone acetylation data improve prediction of mammalian transcription factor binding sites. *Bioinformatics* 2010, 26: 2071–2075.

58. Pique-Regi R, Degner JF, Pai AA, Gaffney DJ, Gilad Y, Pritchard JK. Accurate inference of transcription factor binding from DNA sequence and chromatin accessibility data. *Genome Res* 2010, 21:447–455.

59. Cuellar-Partida G, Buske FA, McLeay RC, Whitington T, Noble WS, Bailey TL. Epigenetic priors for identifying active transcription factor binding sites. *Bioinformatics* 2011, 28:56–62.

60. Lynn DJ, Winsor GL, Chan C, Richard N, Laird MR, Barsky A, Gardy JL, Roche FM, Chan TH, Shah N, et al. InnateDB: facilitating systems-level analyses of the mammalian innate immune response. *Mol Syst Biol* 2008, 4:218.

61. Heng TS, Painter MW. The Immunological Genome Project: networks of gene expression in immune cells. *Nat Immunol* 2008, 9:1091–1094.

62. Robert C, Lu X, Law A, Freeman TC, Hume DA. Macrophages.com: an on-line community resource for innate immunity research. *Immunobiology* 2011, 216: 1203–1211.

63. Raza S, McDerment N, Lacaze PA, Robertson K, Watterson S, Chen Y, Chisholm M, Eleftheriadis G, Monk S, O'Sullivan M, et al. Construction of a large scale integrated map of macrophage pathogen recognition and effector systems. *BMC Syst Biol* 2010, 4:63.

64. Cavalieri D, Rivero D, Beltrame L, Buschow SI, Calura E, Rizzetto L, Gessani S, Gauzzi MC, Reith W, Baur A, et al. DC-ATLAS: a systems biology resource to dissect receptor specific signal transduction in dendritic cells. *Immunome Res* 2010, 6:10.

Cell Host & Microbe
Article

Lipocalin 2 Bolsters Innate and Adaptive Immune Responses to Blood-Stage Malaria Infection by Reinforcing Host Iron Metabolism

Hong Zhao,[1] Aki Konishi,[1] Yukiko Fujita,[1] Masanori Yagi,[2] Keiichi Ohata,[1] Taiki Aoshi,[3,6] Sawako Itagaki,[2] Shintaro Sato,[7] Hirotaka Narita,[4] Noha H. Abdelgelil,[5] Megumi Inoue,[8,9] Richard Culleton,[8] Osamu Kaneko,[9] Atsushi Nakagawa,[4] Toshihiro Horii,[2] Shizuo Akira,[5] Ken J. Ishii,[3,6] and Cevayir Coban[1,*]
[1]Laboratory of Malaria Immunology, Immunology Frontier Research Center (IFReC)
[2]Department of Molecular Protozoology, Research Institute for Microbial Diseases
[3]Laboratory of Vaccine Science, IFReC
[4]Laboratory of Supramolecular Crystallography, Institute for Protein Research
[5]Laboratory of Host Defense, IFReC
Osaka University, 3-1 Yamadaoka, Suita, Osaka 565-0871, Japan
[6]Laboratory of Adjuvant Innovation, National Institute of Biomedical Innovation (NIBIO), 7-6-8 Saito-Asagi, Ibaraki, Osaka 567-0085, Japan
[7]Division of Mucosal Immunology, Department of Microbiology and Immunology, Institute of Medical Science, University of Tokyo, Tokyo 108-8639, Japan
[8]Malaria Unit
[9]Department of Protozoology
Institute of Tropical Medicine (NEKKEN) and the Global COE Program, Nagasaki University, Nagasaki 852-8523, Japan
*Correspondence: ccoban@biken.osaka-u.ac.jp
http://dx.doi.org/10.1016/j.chom.2012.10.010

SUMMARY

Plasmodium parasites multiply within host erythrocytes, which contain high levels of iron, and parasite egress from these cells results in iron release and host anemia. Although *Plasmodium* requires host iron for replication, how host iron homeostasis and responses to these fluxes affect *Plasmodium* infection are incompletely understood. We determined that Lipocalin 2 (Lcn2), a host protein that sequesters iron, is abundantly secreted during human (*P. vivax*) and mouse (*P. yoelii*NL) blood-stage malaria infections and is essential to control *P. yoelii*NL parasitemia, anemia, and host survival. During infection, Lcn2 bolsters both host macrophage function and granulocyte recruitment and limits reticulocytosis, or the expansion of immature erythrocytes, which are the preferred target cell of *P. yoelii*NL. Additionally, a chronic iron imbalance due to Lcn2 deficiency results in impaired adaptive immune responses against *Plasmodium* parasites. Thus, Lcn2 exerts antiparasitic effects by maintaining iron homeostasis and promoting innate and adaptive immune responses.

INTRODUCTION

Iron is an essential nutrient required by all microbial organisms for growth. Many pathogenic microorganisms possess the ability to manipulate their host's iron metabolism in order to acquire sufficient iron for their own growth. Healthy mammals recycle the majority (~95%) of serum iron that is released from the destruction of aged erythrocytes. However, this fine balance is often altered during microbial infection (Hentze et al., 2004; Nairz et al., 2010; Wang and Pantopoulos, 2011). The immune system's response to infectious diseases in the context of iron status is rather complex and poorly understood. For instance, while iron deficiency has been reported to be a predictor of increased susceptibility to many microbial infections (Oppenheimer, 2001), iron overload has been shown to exacerbate several microbial diseases including tuberculosis and salmonellosis (Gangaidzo et al., 2001; Schaible and Kaufmann, 2004).

In the case of malaria, an iron supplementation trial in Tanzania indicated that iron supplementation might increase the morbidity and mortality of children suffering from malarial anemia (Sazawal et al., 2006), while iron deficiency itself has been linked with some degree of resistance to the disease (Matsuzaki-Moriya et al., 2011; Nyakeriga et al., 2004). During their blood-stage life cycle, *Plasmodium* parasites grow and multiply within erythrocytes (an abundant source of iron-containing hemoglobin), which are destroyed in large numbers during parasite egress. This destruction of erythrocytes is associated with the release of heme/iron (along parasite-derived factors) from the ruptured cells. However, the interactions between *Plasmodium* parasites and host iron status during malaria infection have not been examined thoroughly (Prentice, 2008).

Very little is currently known about the parasite's manipulation of iron homeostasis during liver and blood stage malarial infection. Hepcidin, an iron-regulating small peptide mainly expressed in liver, has recently been reported to be important in controlling the iron levels of the host during infection, thereby changing iron availability for *Plasmodium* parasites (de Mast et al., 2009; Portugal et al., 2011; Wang et al., 2011). Compelling evidence suggests that there are yet other factors that influence the ability of pathogens to acquire iron from their hosts. In bacterial infections, bacterial siderophores (i.e., enterobactin) are used

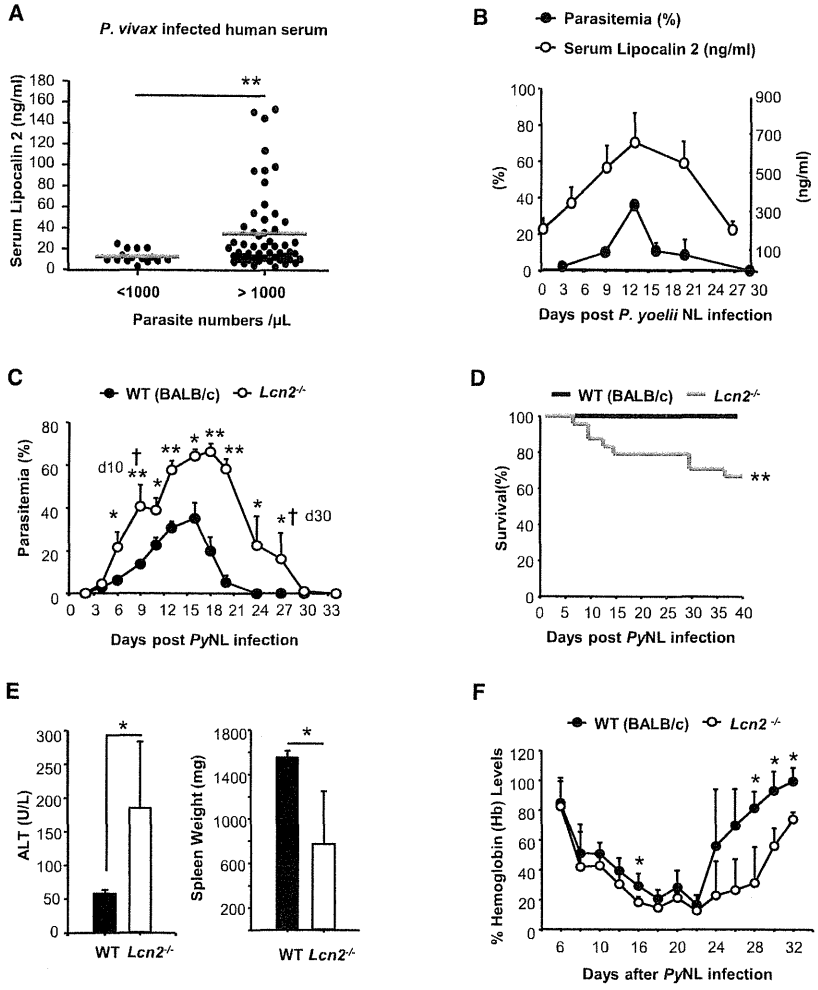

Figure 1. *Plasmodium* Infection Induces Lipocalin 2 Secretion by Host

(A) Serum Lcn2 protein levels in *P. vivax*-infected human serum were measured by ELISA. *P. vivax*-infected patients were divided into two groups according to parasite densities in their blood; patients with parasite densities less than 1,000 parasites/μl (n = 15) and patients with heavy parasitemia (>1,000 parasites/μl of blood) (n = 54). Gray lines show the mean Lcn2 levels of individuals. **p < 0.01 by Mann-Whitney test.

(B) Kinetics of parasite burden and serum Lcn2 levels of mice (BALB/c, n = 7) infected with 10^5 *Py*NL-infected erythrocytes. Percent parasitemia was assessed from blood smears. Serum Lcn2 protein levels were measured by ELISA. Data are represented as mean ± SD.

(C) WT (BALB/c, n = 10) and *Lcn2*$^{-/-}$ (n = 7) mice were infected i.p. with 10^5 *Py*NL-infected erythrocytes, and parasite levels were assessed at the indicated time points. Data are represented as mean ± SD, *p < 0.05 and **p < 0.01 by Mann-Whitney test. † indicates the time of death.

(D) Survival curves of WT (n = 23) and *Lcn2*$^{-/-}$ (n = 24) mice after infection with 10^5 *Py*NL-infected erythrocytes. The survival was monitored daily. **p = 0.0026, log-rank (Mantel-Cox) test.

(E) Serum ALT levels were measured and spleens were weighed at the time of peak parasitemia on day 13 after infection. Data are represented as mean ± SD, n = 3 per group, *p < 0.05 by Student's t test.

(F) Blood hemoglobin levels in WT and *Lcn2*$^{-/-}$ mice during infection were measured in fresh blood taken every other day. Data are represented as mean ± SD, n = 6 per group, *p < 0.05 by Mann-Whitney test. For (E) and (F), data are representative of at least two different experiments. See also Table S1.

to sequester iron from the host. In turn, the host releases a siderocalin, Lcn2, for the inhibition of siderophore-mediated iron acquisition (Bachman et al., 2009; Bao et al., 2010; Flo et al., 2004; Saiga et al., 2008). Lcn2 (also called siderocalin, neutrophil gelatinase-associated lipocalin [NGAL], or 24p3) is a member of the lipocalin family of soluble proteins and was originally identified as a constituent of specific granules found in human neutrophils (Kjeldsen et al., 1993). However, Lcn2 is a multifunctional protein, which has been found to mediate several biological processes, including delivery of iron and fatty acids as well as induction of apoptosis (Chu et al., 1998; Yang and Moses, 2009). It has also been shown that Lcn2 expression can be induced by oxidative stress, hypoxia, and anemia (Jiang et al., 2008; Roudkenar et al., 2007). Furthermore, Lcn2 plays a role in hematopoiesis where it inhibits hematopoietic erythroid and monocyte/macrophage lineages and their differentiation both in humans and mice (Miharada et al., 2005, 2008).

As we have previously demonstrated that Lcn2 is upregulated during malaria infection in mice (Coban et al., 2007b), we hypothesized that it may regulate the interactions between iron homeostasis and the immune system during malaria infection. Our results reveal that Lcn2 has a pivotal role in controlling parasite levels as well as host innate and adaptive responses during *Plasmodium* blood-stage malaria infections and that this role may involve host iron status.

RESULTS

Lipocalin 2 Induced by *Plasmodium* Infection Helps to Control Parasite Growth

To investigate the role of Lcn2 during malaria infection, we measured the serum Lcn2 levels of *P. vivax* patients from southeastern Turkey, where persistent focal *P. vivax* malaria occurs. Study participants (detailed patient information is published elsewhere [Yildiz Zeyrek et al., 2011; Zeyrek et al., 2008] [Table S1]) were divided into two groups according to the parasite load in the blood, as determined by microscopy: patients with fewer than 1,000 parasites/μl of blood (n = 15) and with more than 1,000 parasites/μl of blood (n = 54). We observed significantly higher Lcn2 levels with increasing parasite density (Figure 1A), which suggests that *P. vivax* infection stimulates Lcn2 production.

Plasmodium yoelii nonlethal (*Py*NL) infection in mice has many features in common with *P. vivax* infection in humans (Vigário et al., 2001). To evaluate whether an increase in parasitemia also correlated with higher Lcn2 levels in *Py*NL-infected mice, mice were injected with 10^5 *Py*NL-infected erythrocytes and followed for up to 40 days for parasitemia (expressed as the percentage of infected red blood cells [iRBCs] and serum Lcn2 protein levels). As in the *P. vivax* malaria patients, Lcn2 sera levels were found to increase with parasitemia during blood-stage *Py*NL infection (Figure 1B). Next, *Lcn2*$^{-/-}$ mice were infected and followed throughout the blood-stage course of infection. Infected *Lcn2*$^{-/-}$ mice had significantly higher parasitemia (Figure 1C) with reduced survival (Figure 1D, ** $p < 0.01$) compared to WT control mice. Because liver damage occurs during malaria infection due to higher parasitemia (Haque et al., 2011; Seixas et al., 2009), hepatic function was evaluated by measuring alanine transaminase (ALT) levels. *Lcn2*$^{-/-}$ mice were shown to suffer from hepatic dysfunction (higher ALT levels) compared to WT counterparts during peak parasitemia (Figure 1E). Spleen size was significantly smaller in *Lcn2*$^{-/-}$ mice, suggesting impaired splenic responses (Martin-Jaular et al., 2011; Yap and Stevenson, 1992) (Figure 1E). In addition, the reduced hemoglobin levels in *Lcn2*$^{-/-}$ mice suggest that these mice developed severe anemia during infection and had difficulty recovering from it (Figure 1F). Combined, these data from human and rodent *Plasmodium* infections suggest that Lcn2 is secreted during blood-stage malaria infection and plays a critical role in controlling parasite levels.

Granulocytes, but Not Macrophages, Are the Source of Lipocalin 2 in the Liver and Spleen during *Py*NL Infection

To understand how Lcn2 controls parasite levels, we first sought the source of Lcn2 during blood-stage *Py*NL infection. Spleen and liver macrophages phagocytose and eliminate *Plasmodium*-infected erythrocytes and their metabolites, and the immune responses that occur in the liver and the spleen are of critical importance during malaria infection (Dockrell et al., 1980; Epiphanio et al., 2008; Lau et al., 2001). Lcn2 mRNA transcripts were found to be continuously overexpressed in the livers of mice during the first 10 days of infection, but lowered immediately following peak parasitemia (Figure 2A). In contrast, expression of Lcn2 in the spleen significantly increased during parasite clearance and was sustained for a considerable period (up to 30 days after infection) (Figure 2A). To determine which cell type was predominantly involved in the secretion of Lcn2, we performed immunohistochemical analysis of liver and spleen sections. Very few Lcn2-secreting cells were found in naive liver tissues (data not shown). Lcn2-positive cells were apparent only in liver tissue following *Py*NL infection (Figure 2B). Lcn2-secreting cells colocalized with Gr1$^+$ granulocytes, but not F4/80$^+$ macrophages or hepatocytes (Figures 2B and 2C). Similarly, in the spleen most of the Gr1$^+$ granulocytes colocalized with Lcn2 following *Py*NL infection (Figures 2B and 2C).

We found that the numbers of such infiltrated Gr1$^+$ granulocytes in the livers of *Lcn2*$^{-/-}$animals were significantly reduced at the early stage of infection (day 8, Figure 2D). This was accompanied by a reduction in IFNγ and IL-1β transcripts (Figure 2D). To determine whether granulocytes are the major source and are of primary importance for controlling parasitemia during *Py*NL infection, granulocytes were depleted in vivo by Ly6G-specific antibody (RB6-8C5) 1 day prior to infection via the intravenous route and repeated thrice every 2–3 days. Rat IgG was administrated to mice in the control group. Granulocyte depletion showed a tendency to increase parasitemia; however, this effect was not statistically significant (Figure 2E). Importantly, it did not deplete or reduce serum Lcn2 levels (Figure 2E). Taken together, these findings indicated that liver- and spleen-infiltrating granulocytes produce substantial amounts of Lcn2 at the early as well as late stage of *Py*NL infection and that the infiltration of Lcn2-secreting granulocytes into the liver may play a role in controlling responses to parasites at the early stage of infection. However, the limited effects of granulocyte depletion on serum Lcn2 levels also indicate that there might be other sources of Lcn2, including hematopoietic stem/progenitor cells (Miharada et al., 2005).

Severe Reticulocytosis Occurs in Lipocalin 2-Deficient Mice during *Py*NL Infection

Previous reports have suggested that not only mature granulocytes but also erythroid and monocyte/macrophage lineage cells express and secrete Lcn2 (Miharada et al., 2005). We therefore examined whether erythroid lineage cells are involved in Lcn2 induction or Lcn2-mediated protective immunity during *Py*NL infection. While Lcn2 has been suggested to act as a negative regulator for erythrocytic lineage differentiation (Miharada et al., 2005, 2008), we found no difference in TER119$^+$CD71$^-$ mature erythrocytes in the blood of WT and *Lcn2*$^{-/-}$ mice under normal conditions (data not shown). Upon *Py*NL infection, on the other hand, TER119$^+$CD71$^+$ cells (reticulocytes) increased remarkably up to 20% of RBCs and immediately reduced by the time of parasite clearance in WT mice (Figure 3A). In *Lcn2*$^{-/-}$ mice, reticulocytosis initially was induced similarly to that of WT; however, more robust and sustained numbers of TER119$^+$CD71$^+$ reticulocytes were observed in the blood of *Lcn2*$^{-/-}$ mice on day 22 (~78%, Figure 3A). Of note, these reticulocytes in *Lcn2*$^{-/-}$ mice were infected with *Py*NL parasites (Figure 3B). These data are consistent with the fact that the *Py*NL strain has a strong reticulocyte invasion preference and induces reticulocytosis during infections (Vigário et al., 2001; Yoeli et al., 1975), suggesting that one of the effects of Lcn2 in *Py*NL infection could be to limit reticulocytosis.

To examine whether the enhanced and sustained reticulocytosis in *Lcn2*$^{-/-}$ mice and their persistent infection with *Py*NL parasites leads to severe anemia, total blood cell counts were measured. Infected *Lcn2*$^{-/-}$ mice had significantly lower blood cell counts and higher serum erythropoietin (EPO) levels (Figure 3C), confirming that severe anemia occurred in *Lcn2*$^{-/-}$ mice. Collectively, these data indicate that *Lcn2*$^{-/-}$ mice may develop severe reticulocytosis during *Py*NL infection and that these reticulocytes are persistently infected with parasites, which may result in total blood cell loss and severe anemia.

Lipocalin 2 Controls Extramedullary Erythropoiesis during *Py*NL Infection

We next investigated the relationship between Lcn2 deficiency and *Py*NL-induced reticulocytosis. Previous reports have suggested that Lcn2 inhibits pre-erythrocytic maturation in the

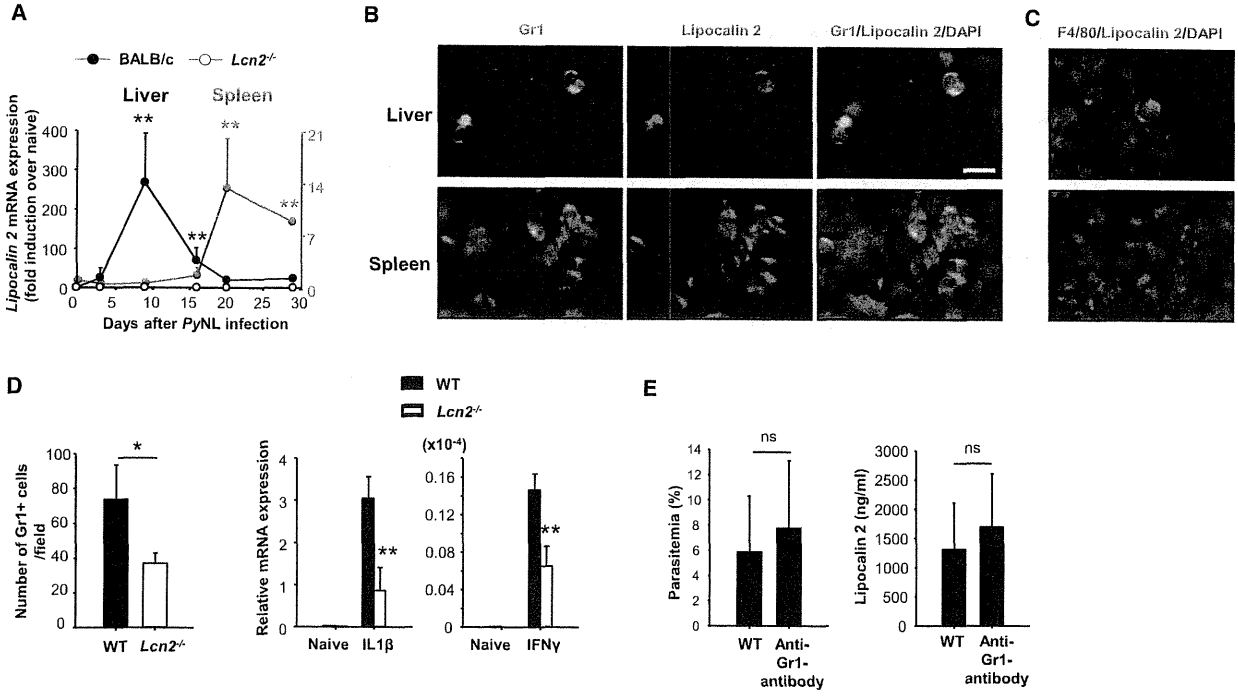

Figure 2. Granulocytes Are the Source of Lcn2 in the Liver and Spleen during *Py*NL Infection

(A) WT (BALB/c) mice were infected with 10^6 *Py*NL, and livers and spleens were removed at the indicated time points. Total RNA was extracted. Expression of Lcn2 mRNA was analyzed by real-time Q-PCR. Results are presented as fold induction over naive mice relative to mRNA units normalized by the corresponding 18S rRNA level. Data are represented as mean ± SD, n = 3 for each time point, $^{**}p \leq 0.01$ for infected WT versus noninfected naive WT mice by Kruskal-Wallis test, whereas Lcn2 mRNA was not detected in *Lcn2*$^{-/-}$ mice.

(B and C) Liver (upper panel) and spleen (lower panel) sections from *Py*NL-infected WT mouse (on day 8 and day 22 postinfection, respectively) were stained with Gr1 (green) and Lcn2 (red) antibodies in (B) and Lcn2 (green) and F4/80 (red) antibodies in (C). Nuclei were visualized by DAPI (blue). The pictures in (B) and (C) are representative of three different animals per time point per group. Images are 400× magnification with scale bar 10 μm and were captured by fluorescence microscope.

(D) Liver sections on day 8 postinfection were stained with anti-Gr1 antibody, and Gr1$^+$ cells were counted by 100× magnification (at least nine sections, three mice per group). Simultaneously, total RNA was extracted. The mRNA levels of IFNγ and IL-1β in livers were analyzed by real-time Q-PCR. Results are presented as relative mRNA units normalized by the corresponding 18S rRNA level (mean ± SD, n = 3 for each time point, $^*p < 0.05$ and $^{**}p < 0.01$ for infected *Lcn2*$^{-/-}$ versus infected WT mice by Student's t test).

(E) Parasite burden and serum Lcn2 levels on day 7 after depletion of Gr1$^+$ cells with RB6-8C5 antibody. Parasitemia was measured from smears, and serum Lcn2 levels were detected by ELISA. Data are represented as mean ± SD, n = 6–8 for each group; ns, not significant.

bone marrow from TER119$^-$ CD71$^-$ to TER119$^-$CD71$^+$ cells and strongly to TER119$^+$CD71$^+$ cells, resulting in controlled production of TER119$^+$CD71$^-$ mature erythrocytes in the blood (Miharada et al., 2005, 2008). The bone marrow and spleen are major sites of erythropoiesis and hematopoiesis during malaria (Crosby, 1983; Del Portillo et al., 2012; Engwerda et al., 2005). Although we observed no differences in erythrocytosis between WT and *Lcn2*$^{-/-}$ mice when uninfected, *Py*NL infection increased extramedullary erythropoiesis significantly in *Lcn2*$^{-/-}$ mice compared to WT mice, and the percentages of TER119$^-$CD71$^+$ as well as TER119$^+$CD71$^+$ cells in the spleen and the bone marrow increased after infection (Figures 4A and 4B). As a result, significantly fewer mature TER119$^+$CD71$^-$ cells were observed in the blood of infected *Lcn2*$^{-/-}$ mice, while WT mice recovered the normal number of mature TER119$^+$CD71$^-$ cells at the same time as they cleared the infection (Figure 4C). Taken together, these results may suggest that severe and sustained reticulocytosis with *Py*NL infection in *Lcn2*$^{-/-}$ mice and the resultant severe anemia may lead to robust extramedullary erythropoiesis in the spleen as well as in the bone marrow.

Lipocalin 2 Reduces Parasitemia through Suppression of Reticulocytosis

To clarify the mechanism by which Lcn2 suppresses parasitemia, we reconstituted *Lcn2*$^{-/-}$ mice with recombinant Lcn2 protein in vivo. Reconstitution of *Lcn2*$^{-/-}$ mice by rLcn2 protein for 6 days after infection reduced parasitemia as well as reticulocyte numbers (Figure 4D). It should be noted, however, that while rLcn2 reconstitution suppressed parasitemia in vivo, rLcn2 had no direct antiparasitic effect under in vitro culture conditions in which *Py*NL parasites were incubated with rLcn2 for 24 hr (Figure 4E).

To further examine whether Lcn2-mediated reduction of parasitemia is due to its effect on the maturation of reticulocytes, we infected WT and *Lcn2*$^{-/-}$ mice with *P. yoelii* Lethal (*Py*L) and *P. berghei* ANKA. While nonlethal *Py*NL parasites mainly infect

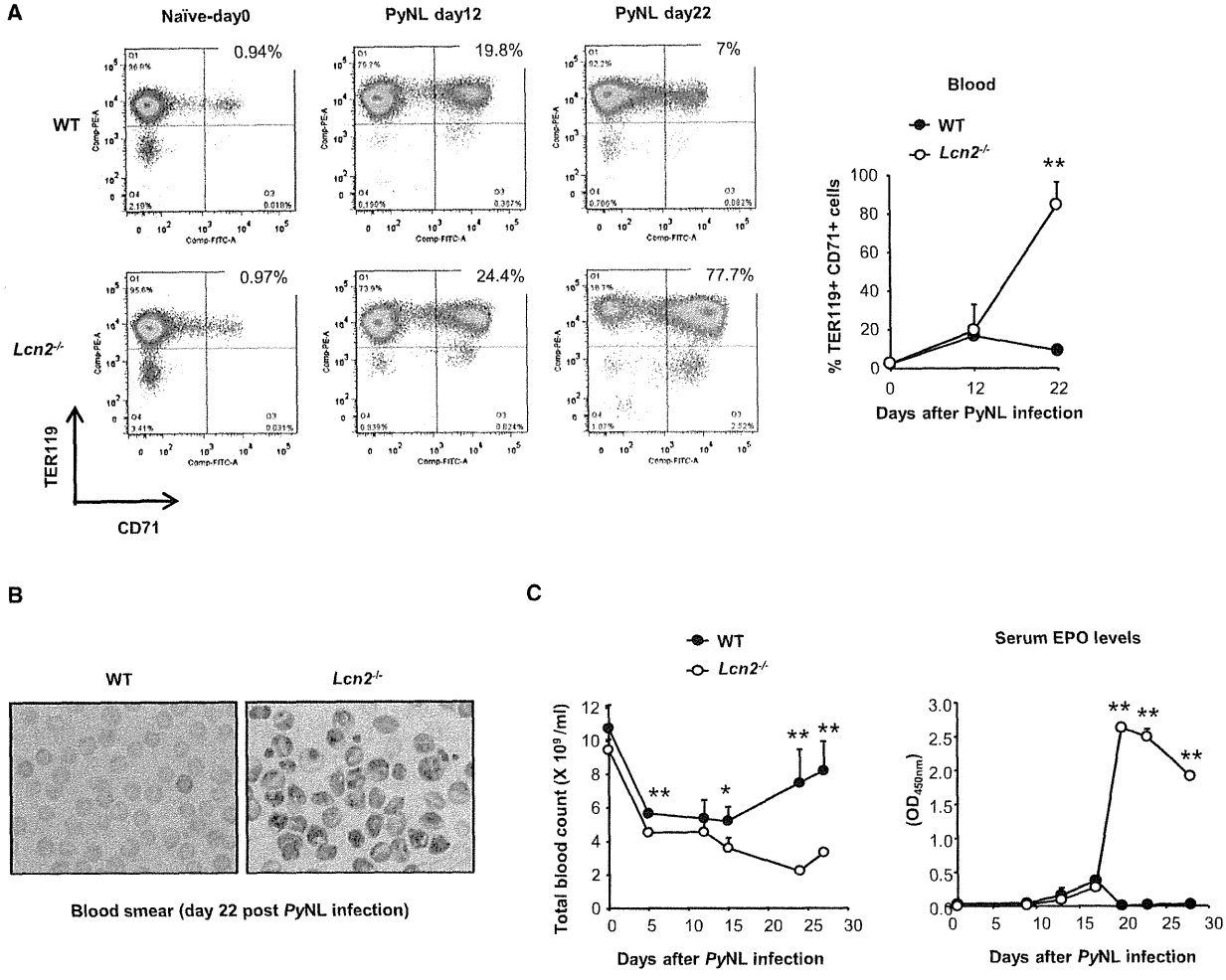

Figure 3. Severe Reticulocytosis Occurs in the Absence of Lcn2 during *Py*NL Infection

(A) Flow cytometric analysis of whole blood on day 12 and day 22 postinfection. WT and *Lcn2*$^{-/-}$ mice were infected i.p. with 10^5 *P. yoelii*NL. Numbers in the upper-right insets show percentages of TER119$^+$CD71$^+$ stained reticulocytes. Figures on the right side show the percentage of TER119$^+$CD71$^+$ cells; data are represented as mean ± SD of three mice per group. **p < 0.01, infected *Lcn2*$^{-/-}$ versus infected WT mice by Student's t test.

(B) Light microscopy of blood smears from WT and *Lcn2*$^{-/-}$ mice stained with Giemsa's solution on day 22 postinfection (1,000× magnification).

(C) Total red blood cell numbers and serum erythropoietin (EPO) levels from WT and *Lcn2*$^{-/-}$ mice at different time points after infection. Total blood cells were counted by cell counter; EPO levels were determined by ELISA. Data are represented as mean OD_{450nm} ± SD, n = 3–5 mice/group for each time point. *p < 0.05 and **p < 0.01, infected *Lcn2*$^{-/-}$ versus infected WT mice by Student's t test.

young erythrocytes, lethal *Py*L parasites infect a wide range of erythrocyte ages and kill hosts rapidly through the induction of acute anemia (Yoeli et al., 1975). *Pb*ANKA parasites infect both mature and immature erythrocytes and cause cerebral malaria, an acute death, due to the sequestration of infected erythrocytes as well as leukocytes in the small vessels such as in brain. Infection of WT and *Lcn2*$^{-/-}$ mice with lethal *Py*L parasites resulted in similar survival rates in the first 10 days of infection with no differences in parasitemia and reticulocytemia (Figure S1A). Similarly, infection of WT and *Lcn2*$^{-/-}$ mice with 10^6 iRBC of *Pb*ANKA parasites caused cerebral malaria symptoms and death within 10 days (Figure S1B; cerebral malaria incidence was ~80% for WT, ~90% for *Lcn2*$^{-/-}$ mice, and 100% for C57BL/6 mice). WT and *Lcn2*$^{-/-}$ mice that did not succumb to cerebral malaria died within 3 weeks of infection due to high parasitemia and resulting anemia, while *Lcn2*$^{-/-}$ mice displayed slightly higher parasite levels (data not shown).

Mice with BALB/c background do not develop CM when infected with *Pb*ANKA, but die due to persistent parasitemia and anemia. Severe reticulocytosis is observed in the latter stages of infection. A different mouse malaria parasite, *P. chabaudi chabaudi*, which also preferentially infects mature erythrocytes, induces reticulocytosis during the recovery phase. *Lcn2*$^{-/-}$ and WT counterparts on BALB/c backgrounds were infected with *Pb*ANKA and *P.c. chabaudi* parasites. The parasitemia and anemia caused by *Pb*ANKA infection was significantly

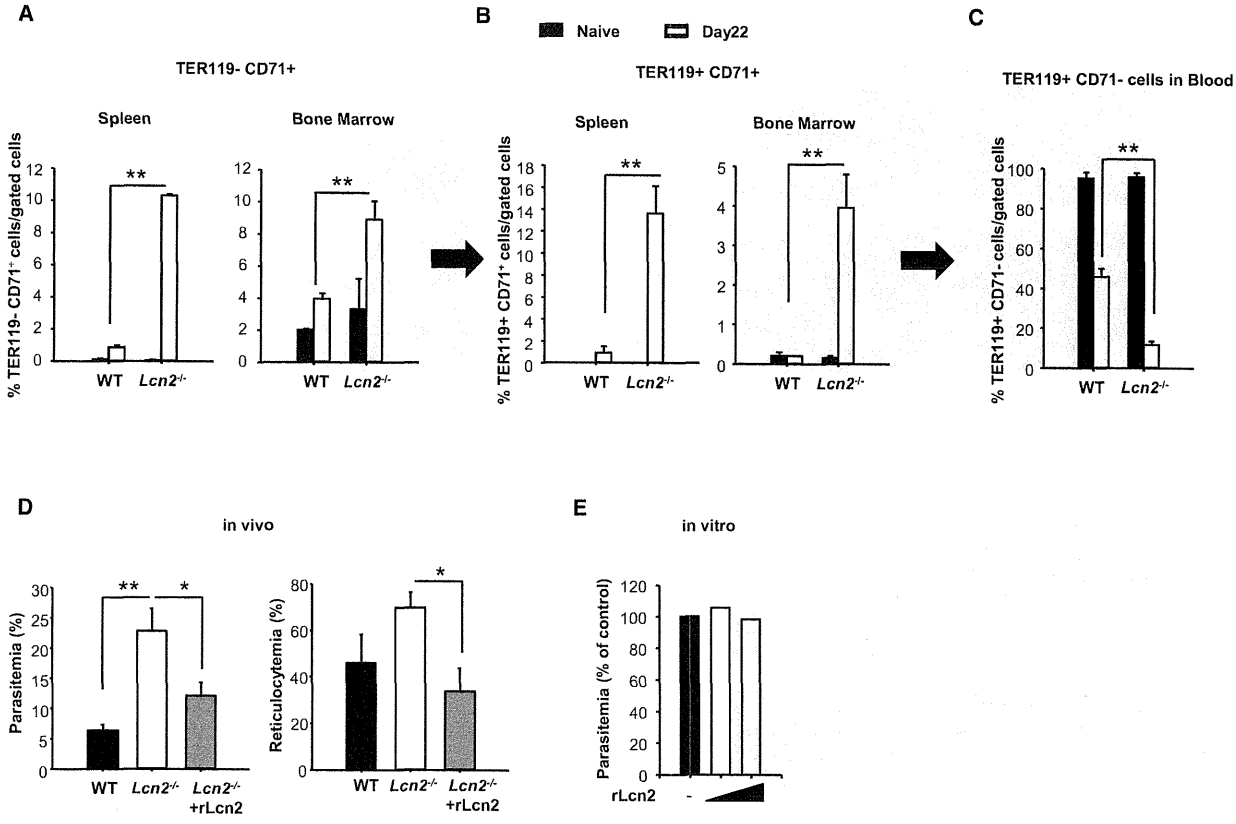

Figure 4. Lipocalin 2 Controls Erythroid Lineage Cell Proliferation in Response to *Py*NL Parasites

(A–C) Whole spleen and bone marrow cells from WT and *Lcn2*$^{-/-}$ mice on day 22 post-*Py*NL infection together with their naive controls were analyzed by flow cytometry. Percentages of TER119$^-$CD71$^+$ cells (A), TER119$^+$CD71$^+$ cells (B), and TER119$^+$CD71$^-$ cells (C) are shown, in spleen and bone marrow (mean ± SD, n = 3 for each group, **p < 0.01 by Student's t test).

(D) *Lcn2*$^{-/-}$ mice were injected daily for 6 days with recombinant mouse Lcn2 protein (150 μg/kg per day). Parasitemia (on day 7) and reticulocytemia (on day 12) were assessed from smears. Data are representative of at least two different experiments (mean ± SD, n = 3–6 for each group, *p ≤ 0.05, **p ≤ 0.01 by Kruskal-Wallis test).

(E) Parasite levels grown in in vitro culture in the presence or absence of mouse rLcn2 protein (1 and 10 μg/ml). Blood was drawn from infected *Lcn2*$^{-/-}$ mice and incubated with rLcn2 protein for 24 hr. Parasitemia was assessed as the % of control group. Data are representative of at least two different experiments. See also Figure S1.

higher during the late stage of infection in *Lcn2*$^{-/-}$ mice compared to WT counterparts, and death occurred earlier (Figures S1C and S1D). *Lcn2*$^{-/-}$ mice infected with *P.c. chabaudi* also had higher parasitemia, reticulocytemia, and anemia than WT control mice (Figures S1E and S1F). Together, these data strongly suggested that Lcn2 plays a critical role in controlling parasitemia during reticulocyte-prone nonlethal *Py*NL infections, possibly through control of reticulocytosis, but does not significantly affect the outcome of mature erythrocyte invading *Plasmodium* infections.

Lipocalin 2 Boosts Macrophage Function and Neutrophil Migration in the Spleen of *Py*NL-Infected Mice

As Lcn2 is expressed in monocyte/macrophage lineages (Miharada et al., 2005), we examined its role in the functions of these cell types during *Py*NL infection. During *Py*NL infection, red pulp F4/80$^+$ macrophages, the major phagocytes of infected erythrocytes, display dramatic changes in spatial and temporal manners (Del Portillo et al., 2012). Splenic red pulp macrophages are the main iron trafficking cells in which heme-oxygenase-1 (HO-1), a heme-catabolyzing enzyme, is involved in the degradation of heme into iron (Kovtunovych et al., 2010; Seixas et al., 2009). In the naive spleen, F4/80$^+$HO-1$^+$ macrophages in the red pulp area were comparable in numbers and localization between WT and *Lcn2*$^{-/-}$ mice (Figures S2A and S2B). However, at day 22 after infection, the cellular changes in the spleens of *Lcn2*$^{-/-}$ mice were severe and sustained (Figure 5A). We found that F4/80 macrophages from *Lcn2*$^{-/-}$ mice displayed a reduction in both HO-1 staining and total *Hmox-1* mRNA expression (Figures 5A–5C), suggesting that macrophage function may be impaired in *Lcn2*$^{-/-}$ mice during *Py*NL infection.

To evaluate whether the phagocytic capacities of splenic macrophages were affected by *Lcn2*$^{-/-}$ deficiency, we investigated the uptake of fluorescent beads by splenic F4/80$^+$ cells during infection. Although the phagocytic capacity of spleen macrophages obtained from uninfected WT and *Lcn2*$^{-/-}$ mice

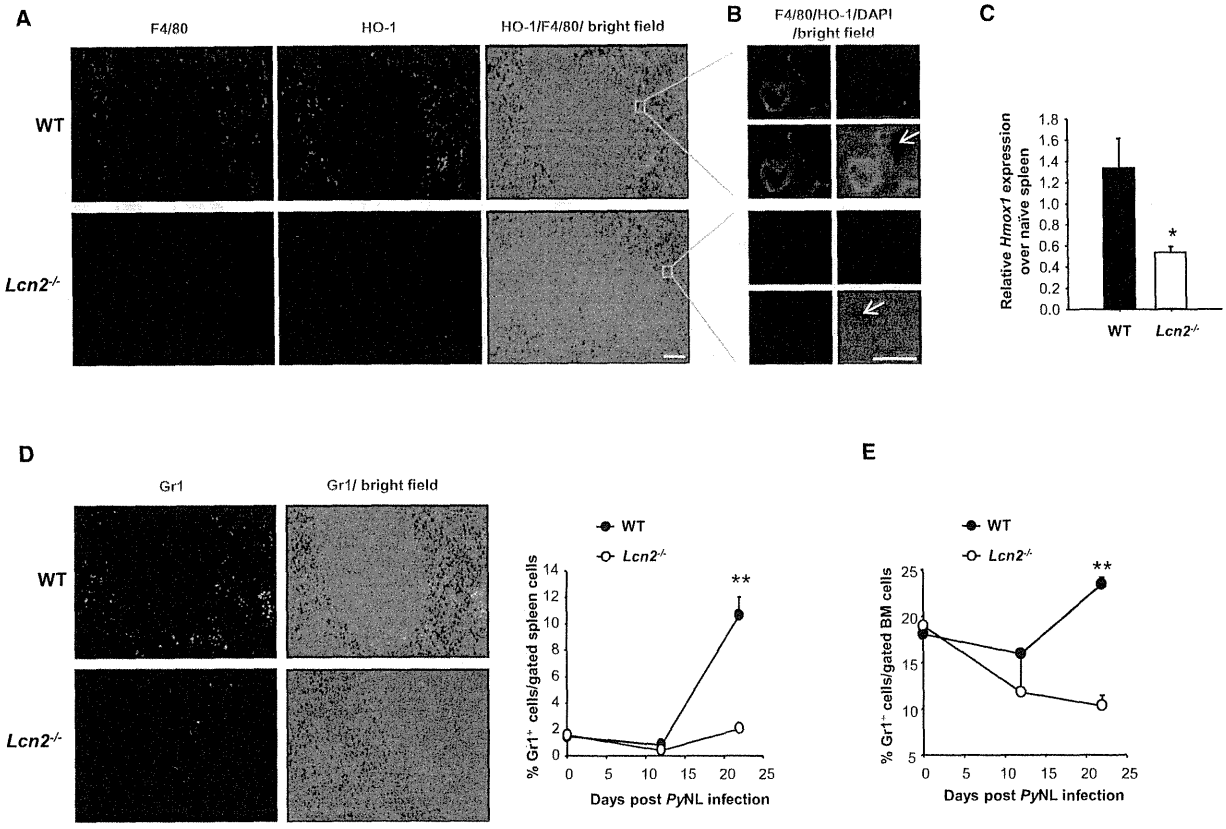

Figure 5. Lipocalin 2 Deficiency Results in Impaired Macrophage Function and Neutrophil Maturation/Migration in the Spleen

(A) Spleen sections from WT and *Lcn2*$^{-/-}$ mice (on day 22 post-*Py*NL infection) were stained with F4/80 (red) and HO-1 (green). Digested hemozoin particles were visualized by bright-field images (100× magnification, scale bar 100 μm).

(B) Insets from red pulp area of (A) are magnified (1,000× magnification, scale bar 10 μm.).

(C) The mRNA levels of *Hmox-1* in spleens were analyzed by real-time Q-PCR on day 22 postinfection. Results are presented as fold induction over naive mice (mean ± SD, *$p < 0.05$, Student's t test, $n = 3$).

(D) Spleen sections on day 22 postinfection were stained with anti-Gr1 (green) antibody. Digested hemozoin particles were visualized by bright-field images (100× magnification). The right-hand figure shows FACS analysis of Gr1$^+$ cells from whole spleens. Data are represented as mean ± SD, $n = 3$ per time point per group, **$p < 0.01$ by Student's t test.

(E) FACS analysis of percent Gr1$^+$ cells from bone marrows on day 22 after infection in WT and *Lcn2*$^{-/-}$ mice (mean ± SD of three mice per group, **$p < 0.01$ by Student's t test). See also Figure S2.

was not significantly different, on day 8 after the infection, spleen weight and percentage of phagocytic F4/80$^+$ cells were significantly lower in *Lcn2*$^{-/-}$ mice (Figures S2C and S2D). Taken together, these data suggest that macrophage function in the spleen, which is a hallmark of recovery from *Py*NL infection, is significantly impaired in the absence of Lcn2. Moreover, while immature granulocyte numbers were increased (Figures S2E and S2F), mature granulocyte numbers in the spleen and BM on day 22 postinfection were greatly reduced in *Lcn2*$^{-/-}$ mice (Figures 5D and 5E), suggesting neutrophil maturation/migration might be impaired in the absence of Lcn2.

Lipocalin 2 Bolsters Iron Recycling and Controls Adaptive Immune Responses to *Py*NL Parasites

The lack of granulocytes/macrophages with the ability to migrate and function optimally during recovery from *Py*NL infection in the absence of Lcn2 prompted us to evaluate iron recirculation; as macrophages are important for recycling host iron via phagocytosis of mature and/or infected erythrocytes (Wang and Pantopoulos, 2011). Furthermore, recovery from anemia is dependent on available iron stores for the production of hemoglobin. As expected, serum iron levels on day 13 postinfection were significantly higher in *Lcn2*$^{-/-}$-infected mice (Figure 6A). Moreover, tissue iron levels in the spleen were significantly reduced in *Lcn2*$^{-/-}$ mice (Figures 6B and 6C). These data indicate that iron recycling was affected by Lcn2 deficiency during *Py*NL infection and that Lcn2 may have a pivotal role in delivering iron to the hematopoietic system.

The transferrin-dependent as well as independent iron acquisition has been shown to be required for T and B lymphocyte proliferation (Cherayil, 2010). Therefore, we investigated whether impaired iron recycling due to Lcn2 deficiency would have an

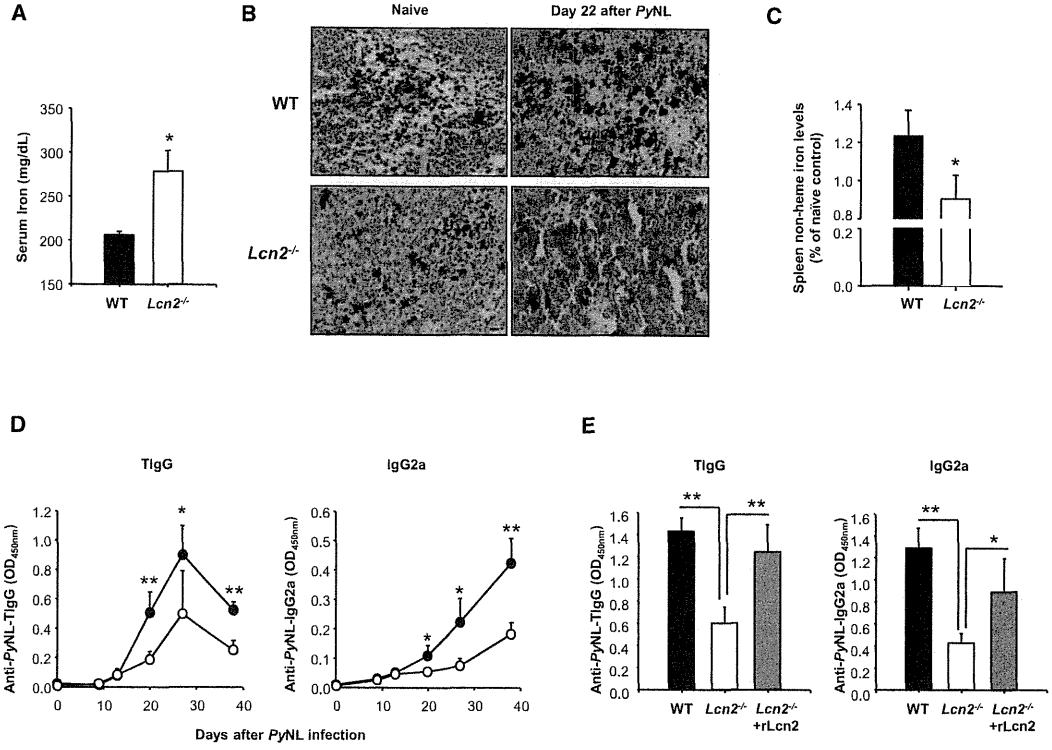

Figure 6. Lipocalin 2 Controls Iron Recycling during *Py*NL Infection, which Helps to Boost Adequate Adaptive Immune Responses to Parasites

(A) Serum iron levels were measured at the peak parasite levels on day 13 after *Py*NL infection. Iron levels are given as mg/ml (mean ± SD, n = 7–10 mice for each group, $^{**}p < 0.05$, by Student's t test).

(B) Spleen sections on day 0 and day 22 postinfection were stained for iron by iron staining kit. Images of sections are 200× magnification.

(C) Total non-heme iron levels of spleens were measured on day 20 after infection. Results are depicted as percentage of naive controls (mean ± SD, n = 4 mice for each group, $^{*}p < 0.05$, by Student's t test).

(D) Parasite-specific antibody responses (total IgG and IgG2a) were measured from serum by ELISA at the indicated time points (mean OD_{450nm} ± SD, n = 15 mice for each group, $^{*}p < 0.05$ and $^{**}p < 0.01$, by Student's t test).

(E) *Lcn2*$^{-/-}$ mice were injected daily with mouse rLcn2 protein for 6 days from the day of infection. Serum parasite-specific total IgG and IgG2a responses were measured by ELISA at day 38 after infection (mean OD_{450nm} ± SD, n = 3–6 mice for each group, $^{*}p \leq 0.05$ and $^{**}p < 0.01$, by Kruskal-Wallis test).

effect on the adaptive immune responses to *Py*NL parasites. Lcn2-deficient animals had an impaired antibody response (*Py*NL-specific total IgG and IgG2a) to *Py*NL parasites (Figure 6D). We confirmed that this was due to Lcn2 deficiency as rLcn2 injection reversed impaired adaptive immune responses to *Py*NL parasites (Figure 6E).

DISCUSSION

For the most pathologically relevant part of their life cycle, malaria parasites invade and divide within erythrocytes, the most abundant source of host hemoglobin in the body. These cells are destroyed in large numbers during parasite egress, an event that is associated with the release of heme/iron into the bloodstream, resulting in a disturbance of iron homeostasis. Lcn2 provides a unique host strategy for competing with bacterial iron chelators (siderophores) for sequestration of iron and confers resistance against various bacterial infections (Chan et al., 2009; Flo et al., 2004; Nairz et al., 2009; Saiga et al., 2008). Here we show that Lcn2 is abundantly secreted into serum during *P. vivax* malaria infection. Due to the limitations of examining the physiological role of Lcn2 upregulation in humans, we evaluated this phenomenon in a mouse model using blood-stage *Py*NL parasites and showed that secreted Lcn2 has a pivotal role in controlling parasite levels and in the successful resolution of the infection. Therefore, current work shows that Lcn2, a unique iron regulator, has a pivotal role in a parasitic disease, through which Lcn2 controls the growth of parasites via modulation of both innate and adaptive immune system.

We report here that one of the major sources of Lcn2 during *Py*NL infection is $Gr1^{+}$ granulocytes accumulated into organs such as the liver (at the early stage) and spleen (at late stage). Granulocytes are known to be activated during malaria infection and to have an eliminating role on malaria parasites (Golenser et al., 1992; Nnalue and Friedman, 1988). Granulocytes can destroy microbes in various ways, such as direct phagocytosis, production of reactive oxygen species (ROS), and through the release of lysosomal components such as enzymes and

antibacterial peptides/proteins (i.e., LL37 and Lcn2). Therefore, in addition to ROS production, it is conceivable that Lcn2 is also secreted from accumulated granulocytes and functions against *Py*NL parasites. Our granulocyte depletion studies, however, revealed that secreted Lcn2 from granulocytes may have a limited role against malaria parasites, as parasite levels were not changed significantly by granulocyte depletion. In addition, granulocyte depletion had no effect on the serum levels of Lcn2. Nevertheless, these findings do not negate the importance of granulocytes on controlling *Py*NL infection, as granulocyte recruitment into livers was partly dependent on Lcn2 (Figure 2D). Although we currently do not know whether Lcn2 plays a direct role in the recruitment of granulocytes into the liver or via secondary effect due to decreased cytokines such as IFNγ or IL-1β, this finding is in agreement with others who show that granulocytes are recruited into inflammation sites in a Lcn2-dependent manner during bacterial or nonbacterial conditions such as spinal cord injury (Bachman et al., 2009; Rathore et al., 2011).

In addition to granulocytes, Lcn2 is likely to be produced from other sources (Miharada et al., 2005). Miharada et al. suggested that erythroid and myeloid lineage cells in bone marrow also express and secrete Lcn2, although it seems to act as a negative regulator for both erythrocytic and myeloid lineage differentiation (Miharada et al., 2008). Lcn2 strongly inhibits pre-erythrocytic maturation from $TER119^{-}CD71^{+}$ cells to $TER119^{+}CD71^{+}$ cells, resulting in controlled production of $TER119^{+}$ mature erythrocytes (over 95%) in the blood. Contrary to expectation, we found no difference in the numbers of $TER119^{+}$ or $TER119^{+}$ $CD71^{+}$ cells in naive WT and *Lcn2*$^{-/-}$ mice (data not shown). However, this changed dramatically in the presence of *Py*NL infection (Figures 3 and 4). It is well known that *Py*NL parasites cause reticulocytosis and have a marked invasion preference for reticulocytes (Yoeli et al., 1975). We found that parasite-induced reticulocytosis was much more severe in the absence of Lcn2, which perhaps in turn caused higher parasite levels. Although reticulocytosis was similarly induced in both groups of mice at the early stage of *Py*NL infection, the percentages of $TER119^{+}CD71^{+}$ cells were remarkably higher in the blood of *Lcn2*$^{-/-}$ animals during the recovery phase (Figure 4B). Having accompanying lower blood cell numbers and higher EPO levels suggested that Lcn2 deficiency caused severe loss of blood and anemia. This conclusion was largely supported by other *Plasmodium* parasites (i.e., *P. berghei*ANKA and *P. chabaudi* infections), which infect both mature and, to some extent, immature erythrocytes.

If Lcn2 affects erythroid lineage differentiation during *Py*NL infection, it is conceivable that Lcn2 affects differentiation of other cell types such as granulocytes. While mature granulocytes ($Gr1^{+}$ cells) in the bone marrow and the spleen during *Py*NL infection were decreased in number until high peak parasitemia in both WT and *Lcn2*$^{-/-}$ mice, their number increased immediately during elimination of parasites only in WT, not in *Lcn2*$^{-/-}$ mice (Figures 5D and 5E). Importantly, severe impairment in the proportion of $Gr1^{high}$ cells in *Lcn2*$^{-/-}$ mice was mirrored by an increase in $Gr1^{low}$ and $Gr1^{int}$ cell proportions (Figure S2), suggesting that granulocyte differentiation may be suppressed during *Py*NL infection. Although this is not seen in uninfected mice, it is possible that the need for rapid proliferation of granulocytes during *Py*NL infection might allow granulocytes to be sensitive to Lcn2-mediated events such as apoptosis (Miharada et al., 2008). This, in turn, may explain lower levels of Lcn2-secreting granulocytes in liver as well as spleen.

A key of our results is that Lcn2 does not exert its antiplasmodial function directly on the parasites, but rather through various indirect mechanisms. Our attempts to show a direct effect of Lcn2 on in vitro *P. falciparum* or *Py*NL cultures failed (data not shown and Figure 4E). It appears that Lcn2 does not simply act on parasitized erythrocytes/reticulocytes, but actually activates other cells such as macrophages during *Py*NL infection. Although macrophages are the target for intracellular pathogens such as *M. tuberculosis* where iron acquisition is influenced (Halaas et al., 2010), the question of how this occurs in malaria infection arises. Macrophages are responsible for the removal of aged erythrocytes and the transfer of degraded heme/iron to the bone marrow for erythropoiesis (Nweneka et al., 2010). Upon phagocytosis of senescent erythrocytes, to efficiently degrade heme and liberate free iron, macrophages increase their expression of HO-1. Liberated free iron is then released efficiently to the circulation through the iron exporters (i.e., ferroportin). Impairment of HO-1 levels may cause inability of macrophage erythrophagocytosis, which may result in intravascular hemolysis, tissue fibrosis, and tissue iron redistribution (Kovtunovych et al., 2010). Our assessment of macrophage function by measuring *Hmox-1* mRNA and protein levels suggests that macrophage function may be impaired during malaria infection if Lcn2 is absent (Figures 5A–5C). One possibility is that Lcn2 might directly induce HO-1 expression and secretion in macrophages (Bahmani et al., 2010; Mori et al., 2005). Therefore, it is plausible that reduced HO-1 levels in macrophages will lead to an increase in free heme and its deleterious products (Seixas et al., 2009). Furthermore, it is possible that a chronic deficiency in the recycling of iron (due to reduced HO-1 activity) via macrophages may suppress macrophage function in a negative feedback manner in the absence of Lcn2. However, given that macrophages can easily modulate adaptive immune responses (Anderson and Mosser, 2002), it is also conceivable that parasite-specific adaptive immune responses were significantly impaired in Lcn2-deficient mice.

We have previously shown that the innate immune system plays a pivotal role in the host's response to malaria parasites in which the MyD88/TLR2/TLR9 axis was found to manipulate the pathology of the disease during infection (Coban et al., 2007a, 2007b, 2010). In addition, we showed that other TLR-related genes such as Lcn2 were also important during malaria infection (Coban et al., 2007b). However, although the protein product of the Lcn2 gene was highly upregulated in the brains of mice following infection by the lethal malaria parasite *P. berghei*ANKA, Lcn2 was not found to be involved in the mortality caused by this parasite (Figure S1B). Presumably, reticulocyte-restricted parasites allow Lcn2 to exert its antimalarial action through the fine balance between anemia, reticulocytosis, and chronic infection and iron recycling.

In summary, we have demonstrated that Lcn2 functions not only as an antimicrobial but also as antiplasmodial defense molecule that exerts its influence by controlling iron redistribution during infection, which in turn is required to recover from malarial anemia and blood loss. We have further demonstrated that

chronic deficiency in iron recycling affects parasite-specific adaptive immune responses to parasites.

EXPERIMENTAL PROCEDURES

Plasmodium vivax-Infected Human Serum

Sixty-nine serum samples from *P. vivax*-infected individuals, as diagnosed by microscopy, were collected in Sanliurfa province in southeastern Turkey and kept at −20°C until use. The details of patients were described elsewhere (Yildiz Zeyrek et al., 2011; Zeyrek et al., 2008) and in Table S1.

All samples were collected after written informed consent was obtained from the patients (or the parents), prior to antimalarial treatment. Sample collection authorization was obtained from the Turkish Ministry of Health, Sanliurfa Bureau, and ethical approval was obtained from the Research Institute for Microbial Diseases, Osaka University.

Mice and Infections

Lcn2$^{-/-}$ mice were generated on a 129/Ola X C57BL/6 (B6.129) background as described previously (Flo et al., 2004) and backcrossed to BALB/c mice (CLEA, Japan) for at least nine generations. Age- and gender-matched wild-type (WT) control BALB/c mice were purchased from CLEA. All animal experiments were conducted in accordance with the guidelines of the Animal Care and Use Committee of Research Institute for Microbial Diseases and Immunology Frontier Research Center of Osaka University.

Donor mice were infected intraperitoneally (i.p.) with *Py*NL-infected erythrocytes; 3–4 days later, blood was drawn, and 10^5 iRBC in 200 μl PBS was inoculated into WT or *Lcn2*$^{-/-}$ mice (i.p.). Parasitemia (expressed as the percentage of infected RBCs) and reticulocytemia (expressed as the percentage of total RBC) were assessed by microscopic counts of Giemsa's solution-stained thin blood smears every 2 days. Blood hemoglobin levels were analyzed using Drabkin's reagent (Sigma), as described elsewhere (Vigário et al., 2001). Total blood cells were counted by a Z1 particle counter (Beckman Coulter, Inc.) from the fresh heparinized blood.

In some experiments *Lcn2*$^{-/-}$ mice were injected with endotoxin-free recombinant Lcn2 protein daily (150 μg/kg per mouse per day, R&D Systems) by the i.p. route for 6 days from the beginning of *Py*NL infection.

Granulocyte Depletion

One day prior to *Py*NL infection, WT (BALB/c) mice were treated with either RB6-8C5 antibody (200 μg, R&D Systems) or rat IgG isotype control by intravenous (i.v.) injection for the depletion of Gr1$^+$ cells. The depletion was repeated every other day thrice. Seven days after infection, parasitemia was assessed and serum was collected for Lcn2 assessment.

Serum ALT and Iron Levels

Serum ALT activity was measured spectroscopically, and serum iron was determined by a direct colorimetric method (Wako, Japan). Spleen tissue non-heme iron levels were measured as described elsewhere (Portugal et al., 2011).

Serum EPO, Lipocalin 2, and Parasite-Specific Antibody Levels

Mouse serum EPO and Lcn2 levels were measured by ELISA (DuoSet ELISA Kit, R&D Systems) according to the manufacturer's instructions. Anti-*Py*NL-specific antibody responses were measured as previously published (Coban et al., 2010).

Flow Cytometric Analysis

Blood, spleens, and bones were collected from mice on the appropriate days, and single-cell suspensions were prepared. Cells were treated with ACK-lysis buffer (Sigma-Aldrich) before staining. All antibodies were from BD Biosciences otherwise mentioned. Cells were FcR-blocked with anti-CD16/CD32 monoclonal antibody prior to staining. Cell surfaces were stained with phycoerythrin (PE)-conjugated anti-TER119, fluorescein isothiocyanate-conjugated (FITC) anti-CD71 (C2), and PE-Cy7 Gr1 (RB6-8C5, Biolegend) antibodies. Samples were acquired on a BD LSRFortessa Flow Cytometer and analyzed with FlowJo software.

Quantitative Real-Time Reverse Transcription-PCR Analysis

Liver and spleen tissues were homogenized, total RNA was isolated with RNAeasy Mini Kits (QIAGEN), and ReverTra Ace (Toyobo) was used for reverse transcription according to the manufacturer's instructions. The cDNA fragments were amplified by Real-Time PCR Master Mix (Toyobo), and fluorescence was detected by a 7500 Real-Time PCR System (Applied Biosystems). The relative induction of each mRNA expression level of each gene was normalized to the expression level of 18S RNA. The primers for 18S rRNA, Lcn2, Hmox1, IFNγ, and IL-1β were purchased from Assays on Demand (Applied Biosystems).

Histopathological Staining of Liver and Spleen

Livers and spleens were removed and fixed with 4% paraformaldehyde (PFA) for 4 hr at 4°C. Samples were then equilibrated in sucrose, embedded in OCT compound (Sakura Finetek, Japan), and kept in liquid nitrogen. Sections were cut with a cryostat (Leica) and mounted onto slides (Matsunami MAS-GP, Japan). After removing the OCT compound in PBS, sections were permeabilized and blocked overnight. Primary antibodies were as follows: anti-mouse Lcn2/NGAL (R&D Systems), PE-F4/80 (BM8, BD Biosciences), FITC-Gr1 (RB6-8C5, BD Biosciences), and HO-1 (Stressgen SPA 895). Secondary antibodies were as follows: Alexa Fluor 594-donkey anti-rat IgG antibody, Alexa Fluor 488-donkey anti-rabbit IgG antibody, and Alexa Fluor 594-donkey anti-rat IgG antibody (Invitrogen). The sections were coverslipped with mounting medium and observed with a fluorescence microscope (Zeiss, Germany). Tissue iron staining was performed by using iron staining kit (Accustain Iron Stain, Sigma).

Statistical Analysis

Differences between two groups were analyzed for statistical significance using a two-tailed, unpaired Student's t test if the data passed normal distribution analysis (Sigma Stat). If not, the statistical significance of differences between two groups was analyzed by a nonparametric Mann-Whitney test. Differences between three groups were analyzed by a Kruskal-Wallis test with Dunn's multiple comparisons. For survival curves, the log-rank (Mantel-Cox) test was performed. $p < 0.05$ was considered statistically significant.

SUPPLEMENTAL INFORMATION

Supplemental Information includes two figures, one table, and Supplemental Experimental Procedures and can be found with this article online at http://dx.doi.org/10.1016/j.chom.2012.10.010.

ACKNOWLEDGMENTS

We thank Dr. Maria M. Mota for insightful discussions and Dr. Fadile Y. Zeyrek for providing serum from *P. vivax*-infected patients in Sanliurfa. We also appreciate the Biken Zaidan laboratories for their help measuring serum iron and ALT levels, Eikoh Gotoh and Mikiko Shimizu for their help in counting parasites from blood smears, and K. Murase and M. Honda for technical support. We greatly appreciate scholarship from Kishimoto Foundation (to H.Z.). This study was supported by grants from the Ministry of Education, Culture, Sports, Science and Technology in Japan and the Osaka University Women Career Design Laboratory Support Service (to C.C.). C.C. and K.J.I. conceived the research. C.C., K.J.I., S.A., T.H., and A.N. oversaw the whole project. H.Z. conducted experiments with help from C.C., Y.F., A.K., T.A., K.O., N.H.A., and S.I.; S.S. made Lipocalin 2-deficient mice; M.Y., H.N., M.I., and R.C. helped with critical experimental design and provided reagents; and C.C., K.J.I., and R.C. wrote the manuscript.

Received: June 15, 2012
Revised: September 3, 2012
Accepted: October 9, 2012
Published: November 14, 2012

REFERENCES

Anderson, C.F., and Mosser, D.M. (2002). Cutting edge: biasing immune responses by directing antigen to macrophage Fc gamma receptors. J. Immunol. *168*, 3697–3701.

Bachman, M.A., Miller, V.L., and Weiser, J.N. (2009). Mucosal lipocalin 2 has pro-inflammatory and iron-sequestering effects in response to bacterial enterobactin. PLoS Pathog. *5*, e1000622.

Bahmani, P., Halabian, R., Rouhbakhsh, M., Roushandeh, A.M., Masroori, N., Ebrahimi, M., Samadikuchaksaraei, A., Shokrgozar, M.A., and Roudkenar, M.H. (2010). Neutrophil gelatinase-associated lipocalin induces the expression of heme oxygenase-1 and superoxide dismutase 1, 2. Cell Stress Chaperones *15*, 395–403.

Bao, G., Clifton, M., Hoette, T.M., Mori, K., Deng, S.X., Qiu, A., Viltard, M., Williams, D., Paragas, N., Leete, T., et al. (2010). Iron traffics in circulation bound to a siderocalin (Ngal)-catechol complex. Nat. Chem. Biol. *6*, 602–609.

Chan, Y.R., Liu, J.S., Pociask, D.A., Zheng, M., Mietzner, T.A., Berger, T., Mak, T.W., Clifton, M.C., Strong, R.K., Ray, P., and Kolls, J.K. (2009). Lipocalin 2 is required for pulmonary host defense against Klebsiella infection. J. Immunol. *182*, 4947–4956.

Cherayil, B.J. (2010). Iron and immunity: immunological consequences of iron deficiency and overload. Arch. Immunol. Ther. Exp. (Warsz.) *58*, 407–415.

Chu, S.T., Lin, H.J., Huang, H.L., and Chen, Y.H. (1998). The hydrophobic pocket of 24p3 protein from mouse uterine luminal fluid: fatty acid and retinol binding activity and predicted structural similarity to lipocalins. J. Pept. Res. *52*, 390–397.

Coban, C., Ishii, K.J., Horii, T., and Akira, S. (2007a). Manipulation of host innate immune responses by the malaria parasite. Trends Microbiol. *15*, 271–278.

Coban, C., Ishii, K.J., Uematsu, S., Arisue, N., Sato, S., Yamamoto, M., Kawai, T., Takeuchi, O., Hisaeda, H., Horii, T., and Akira, S. (2007b). Pathological role of Toll-like receptor signaling in cerebral malaria. Int. Immunol. *19*, 67–79.

Coban, C., Igari, Y., Yagi, M., Reimer, T., Koyama, S., Aoshi, T., Ohata, K., Tsukui, T., Takeshita, F., Sakurai, K., et al. (2010). Immunogenicity of whole-parasite vaccines against Plasmodium falciparum involves malarial hemozoin and host TLR9. Cell Host Microbe *7*, 50–61.

Crosby, W.H. (1983). Hematopoiesis in the human spleen. Arch. Intern. Med. *143*, 1321–1322.

de Mast, Q., Nadjm, B., Reyburn, H., Kemna, E.H., Amos, B., Laarakkers, C.M., Silalye, S., Verhoef, H., Sauerwein, R.W., Swinkels, D.W., and van der Ven, A.J. (2009). Assessment of urinary concentrations of hepcidin provides novel insight into disturbances in iron homeostasis during malarial infection. J. Infect. Dis. *199*, 253–262.

Del Portillo, H.A., Ferrer, M., Brugat, T., Martin-Jaular, L., Langhorne, J., and Lacerda, M.V. (2012). The role of the spleen in malaria. Cell. Microbiol. *14*, 343–355.

Dockrell, H.M., de Souza, J.B., and Playfair, J.H. (1980). The role of the liver in immunity to blood-stage murine malaria. Immunology *41*, 421–430.

Engwerda, C.R., Beattie, L., and Amante, F.H. (2005). The importance of the spleen in malaria. Trends Parasitol. *21*, 75–80.

Epiphanio, S., Mikolajczak, S.A., Gonçalves, L.A., Pamplona, A., Portugal, S., Albuquerque, S., Goldberg, M., Rebelo, S., Anderson, D.G., Akinc, A., et al. (2008). Heme oxygenase-1 is an anti-inflammatory host factor that promotes murine plasmodium liver infection. Cell Host Microbe *3*, 331–338.

Flo, T.H., Smith, K.D., Sato, S., Rodriguez, D.J., Holmes, M.A., Strong, R.K., Akira, S., and Aderem, A. (2004). Lipocalin 2 mediates an innate immune response to bacterial infection by sequestrating iron. Nature *432*, 917–921.

Gangaidzo, I.T., Moyo, V.M., Mvundura, E., Aggrey, G., Murphree, N.L., Khumalo, H., Saungweme, T., Kasvosve, I., Gomo, Z.A., Rouault, T., et al. (2001). Association of pulmonary tuberculosis with increased dietary iron. J. Infect. Dis. *184*, 936–939.

Golenser, J., Kamyl, M., Tsafack, A., Marva, E., Cohen, A., Kitrossky, N., and Chevion, M. (1992). Correlation between destruction of malarial parasites by polymorphonuclear leucocytes and oxidative stress. Free Radic. Res. Commun. *17*, 249–262.

Halaas, O., Steigedal, M., Haug, M., Awuh, J.A., Ryan, L., Brech, A., Sato, S., Husebye, H., Cangelosi, G.A., Akira, S., et al. (2010). Intracellular Mycobacterium avium intersect transferrin in the Rab11(+) recycling endocytic pathway and avoid lipocalin 2 trafficking to the lysosomal pathway. J. Infect. Dis. *201*, 783–792.

Haque, A., Best, S.E., Amante, F.H., Ammerdorffer, A., de Labastida, F., Pereira, T., Ramm, G.A., and Engwerda, C.R. (2011). High parasite burdens cause liver damage in mice following Plasmodium berghei ANKA infection independently of CD8(+) T cell-mediated immune pathology. Infect. Immun. *79*, 1882–1888.

Hentze, M.W., Muckenthaler, M.U., and Andrews, N.C. (2004). Balancing acts: molecular control of mammalian iron metabolism. Cell *117*, 285–297.

Jiang, W., Constante, M., and Santos, M.M. (2008). Anemia upregulates lipocalin 2 in the liver and serum. Blood Cells Mol. Dis. *41*, 169–174.

Kjeldsen, L., Johnsen, A.H., Sengeløv, H., and Borregaard, N. (1993). Isolation and primary structure of NGAL, a novel protein associated with human neutrophil gelatinase. J. Biol. Chem. *268*, 10425–10432.

Kovtunovych, G., Eckhaus, M.A., Ghosh, M.C., Ollivierre-Wilson, H., and Rouault, T.A. (2010). Dysfunction of the heme recycling system in heme oxygenase 1-deficient mice: effects on macrophage viability and tissue iron distribution. Blood *116*, 6054–6062.

Lau, A.O., Sacci, J.B., Jr., and Azad, A.F. (2001). Host responses to Plasmodium yoelii hepatic stages: a paradigm in host-parasite interaction. J. Immunol. *166*, 1945–1950.

Martin-Jaular, L., Ferrer, M., Calvo, M., Rosanas-Urgell, A., Kalko, S., Graewe, S., Soria, G., Cortadellas, N., Ordi, J., Planas, A., et al. (2011). Strain-specific spleen remodelling in Plasmodium yoelii infections in Balb/c mice facilitates adherence and spleen macrophage-clearance escape. Cell. Microbiol. *13*, 109–122.

Matsuzaki-Moriya, C., Tu, L., Ishida, H., Imai, T., Suzue, K., Hirai, M., Tetsutani, K., Hamano, S., Shimokawa, C., and Hisaeda, H. (2011). A critical role for phagocytosis in resistance to malaria in iron-deficient mice. Eur. J. Immunol. *41*, 1365–1375.

Miharada, K., Hiroyama, T., Sudo, K., Nagasawa, T., and Nakamura, Y. (2005). Lipocalin 2 functions as a negative regulator of red blood cell production in an autocrine fashion. FASEB J. *19*, 1881–1883.

Miharada, K., Hiroyama, T., Sudo, K., Danjo, I., Nagasawa, T., and Nakamura, Y. (2008). Lipocalin 2-mediated growth suppression is evident in human erythroid and monocyte/macrophage lineage cells. J. Cell. Physiol. *215*, 526–537.

Mori, K., Lee, H.T., Rapoport, D., Drexler, I.R., Foster, K., Yang, J., Schmidt-Ott, K.M., Chen, X., Li, J.Y., Weiss, S., et al. (2005). Endocytic delivery of lipocalin-siderophore-iron complex rescues the kidney from ischemia-reperfusion injury. J. Clin. Invest. *115*, 610–621.

Nairz, M., Theurl, I., Schroll, A., Theurl, M., Fritsche, G., Lindner, E., Seifert, M., Crouch, M.L., Hantke, K., Akira, S., et al. (2009). Absence of functional Hfe protects mice from invasive Salmonella enterica serovar Typhimurium infection via induction of lipocalin-2. Blood *114*, 3642–3651.

Nairz, M., Schroll, A., Sonnweber, T., and Weiss, G. (2010). The struggle for iron - a metal at the host-pathogen interface. Cell. Microbiol. *12*, 1691–1702.

Nnalue, N.A., and Friedman, M.J. (1988). Evidence for a neutrophil-mediated protective response in malaria. Parasite Immunol. *10*, 47–58.

Nweneka, C.V., Doherty, C.P., Cox, S., and Prentice, A. (2010). Iron delocalisation in the pathogenesis of malarial anaemia. Trans. R. Soc. Trop. Med. Hyg. *104*, 175–184.

Nyakeriga, A.M., Troye-Blomberg, M., Dorfman, J.R., Alexander, N.D., Bäck, R., Kortok, M., Chemtai, A.K., Marsh, K., and Williams, T.N. (2004). Iron deficiency and malaria among children living on the coast of Kenya. J. Infect. Dis. *190*, 439–447.

Oppenheimer, S.J. (2001). Iron and its relation to immunity and infectious disease. J. Nutr. *131* (2S-2), 616S–633S, discussion 633S–635S.

Portugal, S., Carret, C., Recker, M., Armitage, A.E., Gonçalves, L.A., Epiphanio, S., Sullivan, D., Roy, C., Newbold, C.I., Drakesmith, H., and Mota, M.M. (2011). Host-mediated regulation of superinfection in malaria. Nat. Med. *17*, 732–737.

Prentice, A.M. (2008). Iron metabolism, malaria, and other infections: what is all the fuss about? J. Nutr. *138*, 2537–2541.

Rathore, K.I., Berard, J.L., Redensek, A., Chierzi, S., Lopez-Vales, R., Santos, M., Akira, S., and David, S. (2011). Lipocalin 2 plays an immunomodulatory role and has detrimental effects after spinal cord injury. J. Neurosci. *31*, 13412–13419.

Roudkenar, M.H., Kuwahara, Y., Baba, T., Roushandeh, A.M., Ebishima, S., Abe, S., Ohkubo, Y., and Fukumoto, M. (2007). Oxidative stress induced lipocalin 2 gene expression: addressing its expression under the harmful conditions. J. Radiat. Res. (Tokyo) *48*, 39–44.

Saiga, H., Nishimura, J., Kuwata, H., Okuyama, M., Matsumoto, S., Sato, S., Matsumoto, M., Akira, S., Yoshikai, Y., Honda, K., et al. (2008). Lipocalin 2-dependent inhibition of mycobacterial growth in alveolar epithelium. J. Immunol. *181*, 8521–8527.

Sazawal, S., Black, R.E., Ramsan, M., Chwaya, H.M., Stoltzfus, R.J., Dutta, A., Dhingra, U., Kabole, I., Deb, S., Othman, M.K., and Kabole, F.M. (2006). Effects of routine prophylactic supplementation with iron and folic acid on admission to hospital and mortality in preschool children in a high malaria transmission setting: community-based, randomised, placebo-controlled trial. Lancet *367*, 133–143.

Schaible, U.E., and Kaufmann, S.H. (2004). Iron and microbial infection. Nat. Rev. Microbiol. *2*, 946–953.

Seixas, E., Gozzelino, R., Chora, A., Ferreira, A., Silva, G., Larsen, R., Rebelo, S., Penido, C., Smith, N.R., Coutinho, A., and Soares, M.P. (2009). Heme oxygenase-1 affords protection against noncerebral forms of severe malaria. Proc. Natl. Acad. Sci. USA *106*, 15837–15842.

Vigário, A.M., Belnoue, E., Cumano, A., Marussig, M., Miltgen, F., Landau, I., Mazier, D., Gresser, I., and Rénia, L. (2001). Inhibition of Plasmodium yoelii blood-stage malaria by interferon alpha through the inhibition of the production of its target cell, the reticulocyte. Blood *97*, 3966–3971.

Wang, J., and Pantopoulos, K. (2011). Regulation of cellular iron metabolism. Biochem. J. *434*, 365–381.

Wang, H.Z., He, Y.X., Yang, C.J., Zhou, W., and Zou, C.G. (2011). Hepcidin is regulated during blood-stage malaria and plays a protective role in malaria infection. J. Immunol. *187*, 6410–6416.

Yang, J., and Moses, M.A. (2009). Lipocalin 2: a multifaceted modulator of human cancer. Cell Cycle *8*, 2347–2352.

Yap, G.S., and Stevenson, M.M. (1992). Plasmodium chabaudi AS: erythropoietic responses during infection in resistant and susceptible mice. Exp. Parasitol. *75*, 340–352.

Yildiz Zeyrek, F., Palacpac, N., Yuksel, F., Yagi, M., Honjo, K., Fujita, Y., Arisue, N., Takeo, S., Tanabe, K., Horii, T., et al. (2011). Serologic markers in relation to parasite exposure history help to estimate transmission dynamics of Plasmodium vivax. PLoS ONE *6*, e28126.

Yoeli, M., Hargreaves, B., Carter, R., and Walliker, D. (1975). Sudden increase in virulence in a strain of Plasmodium berghei yoelii. Ann. Trop. Med. Parasitol. *69*, 173–178.

Zeyrek, F.Y., Babaoglu, A., Demirel, S., Erdogan, D.D., Ak, M., Korkmaz, M., and Coban, C. (2008). Analysis of naturally acquired antibody responses to the 19-kd C-terminal region of merozoite surface protein-1 of Plasmodium vivax from individuals in Sanliurfa, Turkey. Am. J. Trop. Med. Hyg. *78*, 729–732.

International Reviews of Immunology, 32:209–220, 2013

ISSN: 0883-0185 print / 1563-5244 online
DOI: 10.3109/08830185.2013.773326

informa
healthcare

REVIEW ARTICLE

Particulate Adjuvant and Innate Immunity: Past Achievements, Present Findings, and Future Prospects

Etsushi Kuroda,[1] Cevayir Coban,[2] and Ken J Ishii[1,3]

[1]*Laboratory of Vaccine Science, WPI Immunology Frontier Research Center (IFReC), Osaka University, Suita, Osaka, Japan;* [2]*Laboratory of Malaria Immunology, IFReC, Osaka University, Suita, Osaka, Japan;* [3]*Laboratory of Adjuvant Innovation, National Institute of Biomedical Innovation, Ibaraki, Osaka, Japan*

Particulates and crystals stimulate the immune system to induce inflammatory responses. Several nanometer- to micrometer-sized particulates, such as particle matter 2.5 (PM2.5), diesel particles, and sand dust, induce pulmonary inflammation and allergic asthma. Conversely, nanometer- to micrometer-sized crystal, sphere, and hydrogel forms of aluminum salts (referred to as "alum") have been used as vaccine adjuvants to enhance antibody responses in animals and humans. Although most of these particulates induce type-2 immune responses *in vivo*, the molecular and immunological mechanisms of action as a vaccine adjuvant are poorly understood. In this review, recent advances in particulate adjuvant research from the standpoint of innate immune responses are discussed.

Keywords adjuvant, alum, innate immunity, particulates, vaccine

INTRODUCTION: ADJUVANT AND INNATE IMMUNITY

Immune responses are categorized into two types: innate and adaptive. Innate immunity is mediated by macrophages and dendritic cells (DCs), which engulf and kill microbes. In contrast, adaptive immunity involves antigen-specific responses mediated by T cells, B cells, and memory cells. It had long been believed that the innate immune response functions as a temporal defense system against infection until the adaptive immune response can be elicited. However, recent studies have demonstrated that innate immunity is essential for the effective induction of adaptive immunity [1–3].

Vaccination mimics natural infection and induces pathogen-specific adaptive immunity effectively. Typically, vaccines contain two main components: antigens and adjuvants. An adjuvant is a substance that enhances antigen-specific (adaptive) immune responses when used in combination with a specific antigen. An adjuvant is thought to be an activator of innate immunity. In general, innate immune cells recognize pathogen-derived factors [e.g. pathogen-associated molecular patterns

Accepted 1 February 2013.
Address correspondence to Ken J Ishii, Laboratory of Adjuvant Innovation, National Institute of Biomedical Innovation, Ibaraki, Osaka 567-0874, Japan, and Laboratory of Vaccine Science, WPI Immunology Frontier Research Center (IFReC), Osaka University, Suita, Osaka 565-0871, Japan.
E-mail: kenishii@biken.osaka-u.ac.jp

(PAMPs)], through pattern recognition receptors (PRRs) and induce inflammatory responses. There are four classes of PRRs: Toll-like receptors (TLRs), Nod-like receptors (NLRs), RIG-I-like receptors (RLRs), and C-type lectin receptors (CLRs) [4–7]. These receptors "sense" pathogen-derived factors and transduce activating signals into cells, triggering adaptive immunity against pathogens. Therefore, the ligands for PRRs, such as PAMPs and damage-associated molecular patterns (DAMPs), exhibit potent adjuvant properties that elicit adaptive immunity, and PRRs are considered to be receptors for adjuvants [1, 8].

However, the molecular and immunological mechanisms of many adjuvants used clinically (or those under development) have yet to be fully elucidated. For example, oil emulsions (e.g. Freund's adjuvant and MF-59) and saponin-based adjuvants (e.g., QS-21 and ISCOM) exhibit strong adjuvant activities and could be promising candidates as adjuvants for new human vaccines [9, 10], yet no specific PRR(s) is identified.

An increasing number of particulates and nanoparticles have been reported to exhibit adjuvant activity. A well-known and widely used particulate adjuvant is aluminum salts, which is referred to as "alum" [11–13]. The mechanisms of induction of adaptive immunity by alum or a particulate adjuvant are also unclear, even though alum has been used as a human vaccine adjuvant for more than 80 years. The induction of adaptive immunity requires innate immunity. Hence, it has been proposed that particulates can activate innate cells, and that this action is accompanied by the induction of cytokines, chemokines, and other factors.

PARTICULATES AND THE ADJUVANT EFFECT

Several particulates are known to exhibit adjuvant effects in immune responses. Alum selectively stimulates humoral immune responses, especially type-2 helper (Th2) immune responses, which are characterized by the production of interleukin (IL)-4 and IL-5 and the induction of immunoglobulin (Ig) E and IgG1 [11–13]. (In the case of mice, IgG1 is categorized into Th2-dependent antibody, but the IgG isotype for human Th2 responses has not been clarified fully.) Similar to alum, crystalline silica (which causes a type of pulmonary fibrosis referred to as "silicosis") induces Th2 responses and antigen-specific IgE and IgG1 [14]. It has been reported that synthesized particles, such as poly(lactic-co-glycolic acid) (PGLA), polystyrene particles, nickel oxide nanoparticles, and carbon nanotubes, induce humoral immunity, especially antigen-specific production of IgG1 and IgE [15–19]. Several particulate pollutants, such as diesel exhaust particles, have been shown to induce Th2 responses after intratracheal instillation and are thought to be the source of allergic diseases [20, 21]. In addition to artificial particulates, several crystals generated in the body induce inflammatory responses and possess adjuvant activity. Monosodium urate (MSU) crystals are formed if the concentration of uric acid released from damaged cells reaches saturation. MSU crystals act as DAMPs, and are the causative agent of gout. MSU crystals also act as Th2 adjuvants [22–26]. The biocrystalline substance hemozoin is a hemin detoxification byproduct of malaria parasites. Hemozoin exhibits a potent adjuvant effect and induces humoral immune responses [27]. Chitin particles, which are biopolymers of N-acetyl-D-glucosamine found in fungi, helminthes, and insects, induce the accumulation of IL-4-producing eosinophils and basophils, and are associated with allergy [28]. In contrast to PAMPs such as lipopolysaccharide (LPS) and CpG oligodeoxynucleotides, almost all particulates preferentially elicit Th2 responses and the induction of IgE. Therefore, it has been hypothesized that the specific signals evoked by particulates in innate cells are involved in triggering adaptive (Th2) responses.